DOI: 10.1002/smll.200500390

Nanomachining by Colloidal Lithography

Seung-Man Yang, Se Gyu Jang, Dae-Geun Choi, Sarah Kim, and Hyung Kyun Yu*

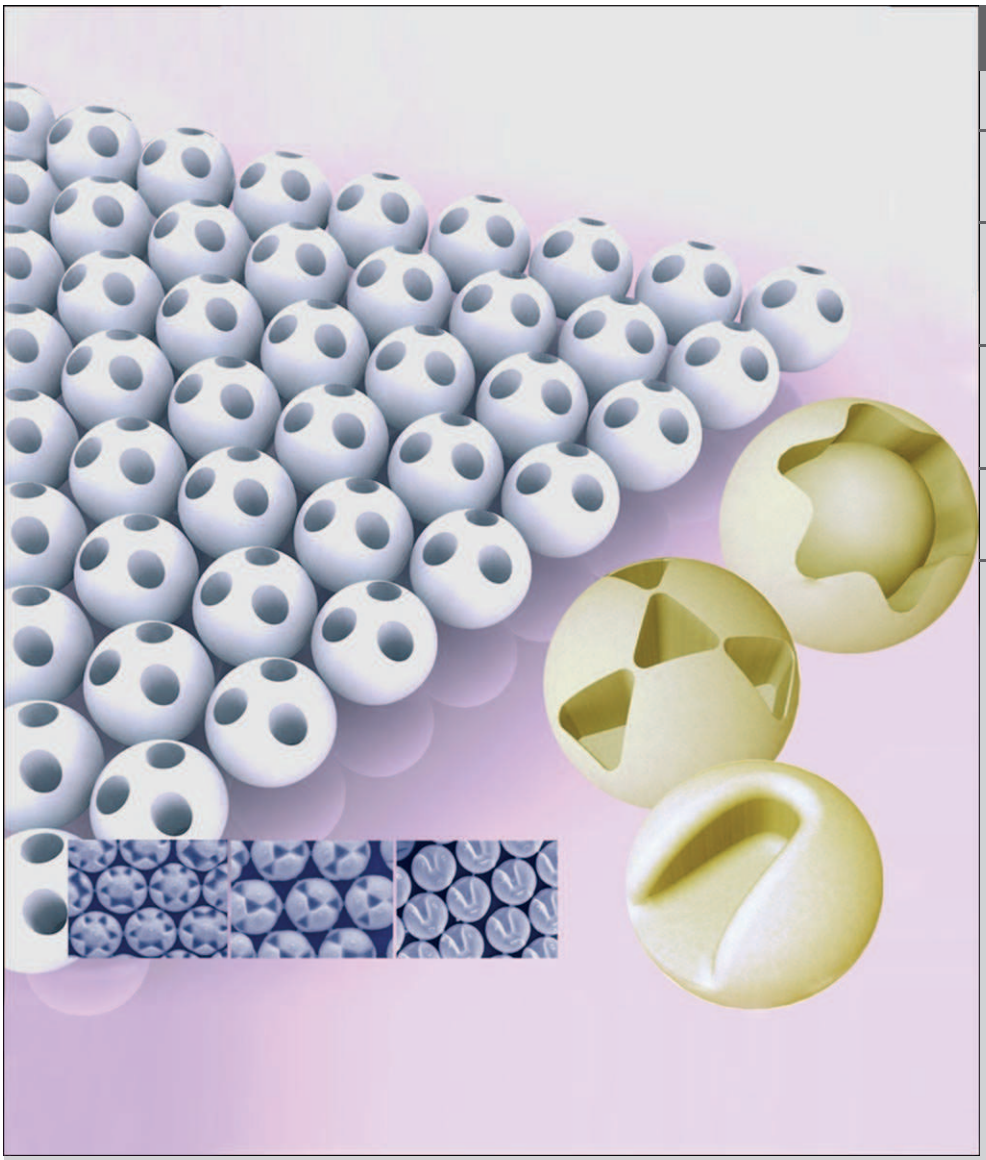

Colloidal lithography is an elegant and emerging technique for creating nanoscale patterns.

NANO MICRO small

From the Contents

1. Introduction.....459
2. Colloidal Particles and their Regular Arrays. 460
3. Colloidal Lithography for Nanopatterned Structures.....463
4. Applications of CL-Assisted Nanopatterns 470
5. Summary and Outlook 473

Keywords:
- colloids
- lithography
- nanomaterials
- patterning
- self-assembly

© 2006 Wiley-VCH Verlag GmbH & Co. KGaA, D-69451 Weinheim

Colloidal lithography is a recently emerging field; the evolution of this simple technique is still in progress. Recent advances in this area have developed a variety of practical routes of colloidal lithography, which have great potential to replace, at least partially, complex and high-cost advanced lithographic techniques. This Review presents the state of the art of colloidal lithography and consists of three main parts, beginning with synthetic routes to monodisperse colloids and their self-assembly with low defect concentrations, which are used as lithographic masks. Then, we will introduce the modification of the colloidal masks using reactive ion etching (RIE), which produces a variety of nanoscopic features and multifaceted particles. Finally, a few prospective applications of colloidal lithography will be discussed.

1. Introduction

Nanolithography is a process for fabricating functional nanostructures from bulk materials. Generally, materials on a nanometer-scale possess unique properties due to their small length scales, low dimensionality, and interactions between neighboring particles. These unexpected properties have provided the motivation for the miniaturization of feature size in many fields such as nanoelectromechanical systems, high-performance catalysis, nanochemicals and biosensors, nanooptical sensors, displays, and nanofluidic devices.[1] In particular, the development of photolithography has been stimulated by the microelectronics industries, and has led to today's microfabrication technologies. The advantages of this technique, such as high resolution and high throughput, allow the preparation of patterns with features of several-hundred nanometers in size. However, conventional photolithography is not suitable on the sub-100 nm scale due to optical resolution limits such as the diffraction of light, backscattering from the substrate, and difficulty in developing the patterns as the scale and critical device dimensions decrease.

Recently, the growing demand for more accurate patterning and higher integration density has stimulated the development of advanced lithographic techniques including immersion lithography, which uses a higher-refractive-index liquid between an imaging lens and a photoresist, and other techniques employing e-beam, scanning probe, and focused ion beams. Details on these advanced lithographic techniques can be found in the literature.[2–4] Although the alternative lithography techniques provide the resolution and integration density required for the industrial demands, the level of throughput rate is far below the industrial requirement. In addition, these advanced developments require very costly instrumentation, and the systems become increasingly delicate due to the addition of compensative processes. Nanoimprint lithography (NIL)[5] and soft lithography[6] have been considered as promising high-throughput patterning techniques, and there has been significant research that has achieved sub-100 nm feature sizes using these techniques. However, both the mold fabrication and the stripping problems remain unsolved, originating mainly from a dramatic increase of surface area on the nanometer scale.

A number of studies have been conducted to develop an alternative lithographic route using building blocks that organize themselves into a well-defined structure. Typical building blocks that have been used widely are block copolymers with the feature sizes ranging from several to a few tens of nanometers. The self-organized structures of these building blocks depend strongly on the interactions between the constitutent blocks.[7–10] These structures are used as masks for the so-called block-copolymer lithography. One of the novel features in these processes is that the building blocks assemble themselves spontaneously in a regular architecture and facile control of an ordered structure can be achieved over a large area without the need for complex equipment.

Colloidal dispersions are heterogeneous systems composed of colloidal particles dispersed in a liquid medium. Recent advances in colloidal science have enabled the synthesis highly monodisperse colloidal particles with good phase stability. Such colloidal particles can be arranged into an array (an ordered structure) through self-organization and have been used as templates for advanced functional materials.[11] In particular, colloidal lithography (CL) uses two-dimensional (2D) arrays of colloid particles as masks for etching or sputtering processes. CL has a few advantages over the aforementioned lithographic techniques: First, CL is a cost-effective process to fabricate nanoscale functional patterns; CL uses a small amount of colloidal dispersion to

[*] Prof. S.-M. Yang, S. G. Jang, S. Kim, H. K. Yu
Department of Chemical and Biomolecular Engineering
Korea Advanced Institute of Science and Technology
373-1 Guseong-dong, Yuseong-gu, Daejeon 305-701 (Korea)
Fax: (+82) 42-869-3910
E-mail: smyang@kaist.ac.kr
Dr. D.-G. Choi
Nano-Mechanical Systems Research Center
Korea Institute of Machinery & Materials
171 Jang-dong, Yuseong-gu, Daejeon 305-343 (Korea)

 © 2006 Wiley-VCH Verlag GmbH & Co. KGaA, D-69451 Weinheim

generate a regular colloid array, and the colloidal dispersions are commercially available at a relatively low cost. Complex equipment is not required to create patterns with features on a scale of several tens of nanometers. Second, CL is a simple process; template formation via self-assembly can be achieved readily by spin-casting or dip-coating. Third, the feature scales in CL are controlled simply by changing the size of the colloidal particles and can be reduced to several tens of nanometers. In particular, some special modifications such as annealing of the particle array or tilted deposition can also modify the feature size. Fourth, three-dimensional (3D) complicated structures can also be fabricated by CL. Materials with designed functional nanopores, hemispherical metal caps and sculptured colloids have been fabricated by colloidal templating for various applications. Fifth and finally, CL is suitable for patterning biomaterials, which are relevant for the fabrication of biosensors or biochips. Generally, the surface of the colloidal particles can be modified readily with biolinkers such as carboxylic acid or amine groups.

CL is a recently emerging field, and the evolution of this simple technique is still ongoing. A variety of experimental tools will yield efficient CL which can replace, at least partly, complex and high-cost advanced lithographic techniques. This Review presents an overview of the recent advances in CL including the methodologies of pattern formation using colloidal particles and its applications. The Review consists of three main sections: First, synthetic routes to monodisperse colloidal particles are discussed, along with the methods used to assemble colloidal templates for preparing lithographic masks. Second, the modification of colloidal masks using reactive ion etching (RIE) is studied. And third, there is an investigation into a few of the prospective applications of the CL-assisted nanopatterns.

2. Colloidal Particles and their Regular Arrays

2.1. Synthetic Methods to Produce Colloidal Particles

Recent efforts to produce monodisperse colloidal particles have led to the development of a number of synthetic routes. Polymer particles such as polystyrene (PS) or poly(methyl methacrylate) (PMMA) beads with a narrow size distribution can be synthesized by suspension, emulsion, dispersion, and precipitation polymerizations.[12] Among them, emulsion and dispersion polymerizations are most commonly used. In particular, emulsifier-free emulsion polymerization has been widely used because the surface properties of the polymeric latexes are controlled by an initiator or comonomers in the absence of an emulsifier.[13] The absence of emulsifiers helps to simplify the synthesis procedure, which requires no removal of the surface-active agents. Many studies have been conducted to control the functional groups of the polymeric beads by using emulsifier-free emulsion copolymerization.[14] In addition to surface functionalization, Zou et al. successfully used emulsion copolymerization to prepare monodisperse crosslinked PS[15a] and PMMA[15b] beads of various sizes with a controllable degree of crosslinking. The synthesized crosslinked polymeric particles were dispersible even in organic solvents. Meanwhile, particle size has been controlled by adjusting the reaction conditions. The reaction temperature and the monomer concentration are the most important factors that control the size of the polymer beads. Because the solubility of the monomer in the aqueous phase depends on temperature and the depletion time of the monomer varies with the monomer concentration, the particle size decreases with an increase in temperature and with a decrease in the monomer concentration. Using these parameters, the size of the polymer beads can be controlled in the range of 100–700 nm using emulsifier-free emulsion polymerization.

For monodisperse polymeric microspheres larger than 1 μm in diameter, the seed polymerization method can be used.[16] After the synthesis of small seed particles, additional repeated polymerizations onto the seed polymer latexes produce larger polymer beads. However, the size distribution of the polymer beads broadens due to the repeated addition of the raw materials. As an alternative for enhanced size uniformity, a single-step dispersion polymerization is generally used for producing larger particles (>1 μm).[17] In dispersion polymerization, the reaction site is a monomer droplet stabilized by a smaller amount of surfactants and an initiator, which is soluble in oil and diffuses to the monomer droplets. Therefore, each monomer droplet acts as a miniature of a bulk polymerization reactor. PS and PMMA microspheres can be synthesized in polar or nonpolar solvents, and surface characteristics and crosslinking density are controlled by copolymerization.[18]

For inorganic metal oxide particles, Stöber et al.[19] developed a technique where, for example, silica particles were prepared using sol–gel chemistry, in which the hydrolysis and condensation of tetraethylorthosilicate (TEOS) proceed in a mixture of alcohol, water, and ammonia. Synthesis of inorganic particles proceeds via two distinguishable steps: nucleation and subsequent growth. For monodisperse particles, these two processes should be separated so that the nuclei can be generated homogeneously without simultaneous growth. After the development of the Stöber method, the sol–gel reaction has been modified by various researchers.[20] Bogush et al.[20b] reported that particle growth occurs primarily through an aggregation mechanism, and small par-

Seung-Man Yang received a PhD degree in Chemical Engineering from Caltech in 1985. Following this, he joined the KAIST as a Professor in Chemical and Biomolecular Engineering. He has served the KAIST as a director of the Computing Center, and a Department Chair. His principal contributions have been in theories and experimental methods for fabricating ordered macrocrystalline structures, which can be applied as innovative functional nanoscopic materials such as optoelectronic devices and biosensors. He has authored over 130 peer-reviewed papers, and a number of books and patents in related areas.

 © 2006 Wiley-VCH Verlag GmbH & Co. KGaA, D-69451 Weinheim

ticles grow faster than larger particles; this phenomenon is known as "self-sharpening". Therefore, the particle size distribution becomes narrower as the reaction proceeds. In general, the size and polydispersity of particles are related to many factors such as pH value, the concentration of catalyst, the composition of reagents, the types of solvents, and the reaction temperature, which all affect the rates of hydrolysis and condensation. Some quantitative reports are available on the effects of these factors controlling the size and polydispersity.[20b,d] The size of monodisperse silica particles can be controlled in the range of 200–600 nm simply by changing the factors described above.

Although silica particles with a narrow size distribution can be synthesized by a single-step growth technique, there are some limitations in increasing the size of particles. In order to synthesize larger silica particles and increase the particle loading, a seeded-growth technique similar to the seeded growth of a polymer has been developed.[20] Silica particles can be dispersed in organic solvents by changing the surface properties with anchored silane coupling agents such as octadecyltrimethoxysilane (OTMOS).[21] The hydrophilic silanol groups (–Si–OH) on the silica surface can then be modified to render the particles hydrophobic.

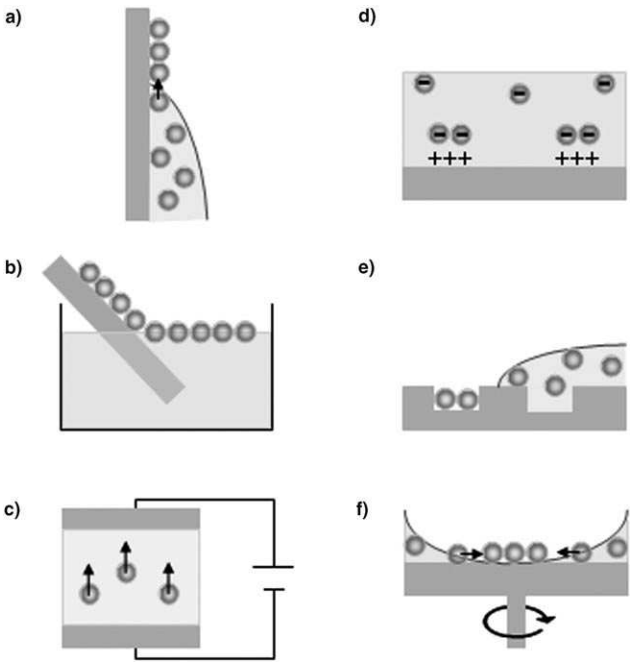

Figure 1. Diverse self-assembly strategies to create ordered colloid arrays: a) dip-coating in which capillary forces and evaporation induce colloidal self-organization, b) lifting up a colloid array from an interface using the substrate, c) electrophoretic deposition of colloids, d) chemical or electrochemical deposition of colloids with a patterned array, e) physical template-guided self-organization of colloids, f) spin-coating in which shear and capillary forces drive the colloidal self-organization.

2.2. Self-Assembly Strategies for Colloid Arrays

Colloidal particles dispersed in various solvents are influenced by interactions including van der Waals forces, steric repulsions, and Coulombic repulsions. Because the dispersion stability and the crystallization of the colloidal dispersion are governed by these interactions, intensive studies on colloidal interactions have been conducted both experimentally and theoretically.[22] Derjaguin–Landau–Vervey–Overbeek (DLVO) theory describes successfully the interactions between colloidal particles and has been used to predict the stabilization of dispersions.[23] However, during the fabrication of colloidal templates or masks for CL, the evaporation of the dispersant solvent induces the self-assembly of the colloidal particles. Under this circumstance, attractive capillary forces play an important role in the ordered arrangement of the colloidal particles. Figure 1 illustrates the typical strategies for fabricating a 2D colloid array including dip-coating, floating on an interface, electrophoretic deposition, physical and chemical template-guided self-assembly, and spin-casting.

Nagayama and co-workers accomplished pioneering work on capillary-force-induced self-ordering of colloidal particles by direct observation of the dynamics of colloids from a random distribution to a 2D hexagonally ordered regular structure via dip-coating.[24] Because attractive capillary forces arise from the formation of a meniscus around the particles, the ordering process starts at the moment when the thickness of the liquid layer of the suspension becomes smaller than the diameter of the particles due to the evaporation of the liquid. Continuous evaporation through the once-formed nuclei results in convective flow of the surrounding suspension, and successive inflow of the colloidal particles to the nuclei is sustained until all of the liquid has evaporated. Figure 1a shows the dip-coating method, in which capillary forces and controlled evaporation induce colloidal self-organization. The quality of the ordered arrays is determined by the evaporation rate, and in general the assembled structure usually has domains throughout the entire area. Control of the evaporation rate has been achieved by a step motor, which helps to lift up the wettable substrate from the colloidal suspension at a very slow rate.[25] Evaporation of the liquid and deposition of the colloids by lateral capillary forces are allowed only at the triple point of the suspension/substrate/air interface. A large-scale polycrystalline monolayer of a colloidal array with a diameter ranging from a few tens of nanometers to a few micrometers can be obtained with this method.

After the development of the dip-coating method, most studies in the self-assembly of colloid arrays have focused on the enhancement of quality, productivity, and controllability of the self-assembled structures. Various methods were proposed to reduce defects such as grain boundaries, dislocations, vacancies, and variations of the thickness of the colloid layers with a simple and rapid process. Self-assembly at the air/liquid or oil/liquid interface, deposition of particles using electrophoresis, and template-assisted self-assembly were applied to fabricate 2D colloid arrays with lower defect densities. In addition, spin-casting was proposed to increase the productivity of the colloid array, which can be formed homogeneously on a wafer scale.

 © 2006 Wiley-VCH Verlag GmbH & Co. KGaA, D-69451 Weinheim

Figure 1b shows the lift-up process of a colloidal array floated on an interface. During the formation of the 2D colloid array at the interface, the quality and packing sequence of the array can be controlled by changing the concentration of the particles or electrolytes, the particle size, the surface charge, and the hydrophobicity of the particles.[26–29] Colloidal particles can be trapped at the liquid interface as a result of electrostatic and capillary forces. For example, a 2D array of silica colloids coated with alkoxyl chains was self-assembled on an air/benzene interface,[26] and a highly ordered monolayer of PS latex particles was formed by long-range repulsive forces between the PS latexes at an octane/water interface, which was induced from the residual surface charges at the particle/octane interface.[28] Furthermore, silica colloids were modified by silanizing the surface to enhance the hydrophobicity and then self-assembled at an octane/water surface. Compared to evaporation-induced self-assembly, the particles at the interface are able to form a monolayer without variation in the layer thickness. As such, a uniform monolayer, as large as several square centimeters, can be obtained by applying the Langmuir–Blodgett film technique.[30] An ordered particle array can be transferred to various substrates by lifting up the colloidal film or by controlled evaporation of the solvent.[26]

Electrophoretic deposition of colloidal particles utilizes the movement of the particles that is driven by applied electrical fields, as shown in Figure 1c. Electrophoretic movement in a dc field[31] or ac field[32] has been studied and applied for rapid and precisely controlled deposition of particles. Particle assembly generally takes place inside a thin layer of a colloidal suspension sandwiched by conducting substrates such as indium tin oxide (ITO) coated glass slides. An electric field is then applied across the electrodes. The driving force assembling the particles into 2D crystals are the electrohydrodynamic interactions between the microspheres.[31,33] Electrophoretic deposition of the particles can be combined with another self-assembly method such as electrophoresis-assisted gravitational sedimentation[34] or template-directed self-assembly.[35] Electrophoretic movement not only accelerates the sedimentation speed of small colloids but also guides the growth of a colloidal crystal over a large area in a controlled manner. Selective deposition of the particles by employing a predesigned pattern was also achieved by Winkleman et al.[36] The patterned electrode was composed of particle-accepting PS domains and particle-repellant gold domains, which differ in their electrostatic interactions with the microspheres.

Template-assisted self-assembly of colloid particles is usually employed for suppressing defect formation in colloidal crystals.[37] A typical example is the selective deposition of colloids on a substrate patterned with chemicals or charges (Figure 1d),[38,39] or a physically patterned substrate (Figure 1e).[40] In particular, the topography of the substrate (e.g., wells and microchannels) can confine the self-assembly of the particles, and the ordering quality and stacking sequence can be controlled by changing the ratio of the particle size to the feature size of the patterned geometry.[36,37] Xia and co-workers have developed a template-assisted growth of colloidal crystals with controllable orientations and features.[40] They fabricated colloidal crystals with facing (100) planes using patterned V-shaped grooves as well as colloidal clusters and helical chain structures by controlled evaporation in a lithographically patterned cylindrical hole array. Similarly, chemical or charge contrast on substrates patterned with self-assembled monolayers (SAMs)[38] or polyelectrolytes[39] can induce the arrangement of colloidal particles into a regularly patterned array. Due to the contrast of the hydrophilicity associated with the chemical contrast of the surface pattern, the particles are deposited selectively on specific regions of the pattern. In the absence of the predesigned patterns, a colloidal monolayer (which was formed due to electrostatic attraction between the colloids and the electrolyte layer) showed a short-range ordering but with a long-range-disordered structure. This random sequential adsorption was predicted by Adamczyk et al. via a Monte Carlo simulation.[39c] Electrostatic attraction of the electrolyte was also employed to fabricate diatomic colloidal clusters for an antireflection coating using layer-by-layer deposition of bidisperse colloidal particles.[39b] Such a coating of bidisperse particles has been investigated intensively due to its potential to form unique packing structures such as non-close-packed or bimodal particle arrays.[41] The degree of coverage and the packing sequence (i.e., LS, LS_2, and LS_3 for stacking sequences of large (L) and small (S) particles) vary dramatically according to the volume fractions and the size ratio of the bidisperse particles.[41a] Controlled drying of a suspension from a certain direction is generally used to reduce defects in the colloidal crystal.

Spin-coating of the particle suspension is also available for preparing the colloidal layer.[41d] During centrifugal spreading of a suspension on a wettable substrate (as shown in Figure 1f), the colloid particles organize themselves into a hexagonal array more rapidly compared to evaporation methods such as dip-coating, drop-dripping, and electrolyte adsorption. In many cases, the wettable substrate exhibits an electrostatic repulsion against the particles. Van Duyne et al. employed spin-coating of a PS latex suspension using a surfactant that enhanced the wettability of the colloidal dispersion to the substrate.[42] The thickness of the particle layer was controlled by adjusting the particle loading and the spin speed. Spin-coating methods have an advantage for both scaling-up and mass production because the spin-coating process is rapid and compatible with wafer-scale processes, which are well established in the area of photolithography. As an example of wafer-scale production, Jiang et al. fabricated well-ordered non-close-packed 2D crystals by the spin-casting of silica particles dispersed in a photocurable polymer matrix.[43] Self-assembly of the particles was achieved within a minute, and the thickness was controlled uniformly on a 4-inch wafer scale. After curing of the polymer through UV exposure with a mask, subsequent removal of the silica particles left behind a patterned array of a polymeric inverse opal.

 © 2006 Wiley-VCH Verlag GmbH & Co. KGaA, D-69451 Weinheim

3. Colloidal Lithography for Nanopatterned Structures

For decades, research trends in nanoscopic patterning have focused on the development of reliable and cost-effective lithographic routes. High efficiency in CL for nanofabrication is due to the fact that large-area spontaneous assembly of a colloid can be produced by the relatively easy methods outlined in Section 2. Self-assembly of a well-ordered structure reduces not only the cost but also the time for nanolithography. CL has attracted a plethora of studies and a variety of lithographic methods have been developed due to their efficiency.

Figure 2 illustrates the representative CL techniques. In the earlier stage of CL, nanometer-scale dot arrays were fabricated using a colloid array as a mask, as shown in Route A of Figure 2. A number of functional materials have been patterned with colloidal masks, which will be discussed in Section 3.1.1. Following numerous studies using simple colloidal masks, shape-tuning of the deposited materials has been conducted to fabricate diverse features in the resultant patterns. As shown in Route B in Figure 2, the structure modifications of the colloidal arrays change the shape of the particles, which in turn control the size and shape of the resulting functional dot arrays. Also, a tilted deposition relative to the substrate or annealing of a colloid mask (as illustrated in Route C of Figure 2) modifies the shape of the deposited materials dramatically. Section 3.1.2 details how the colloidal masks are modified effectively. Recently, photocurable colloids (or photoresist particles) have been utilized to construct hierarchical patterning via CL, as shown in Route D of Figure 2.

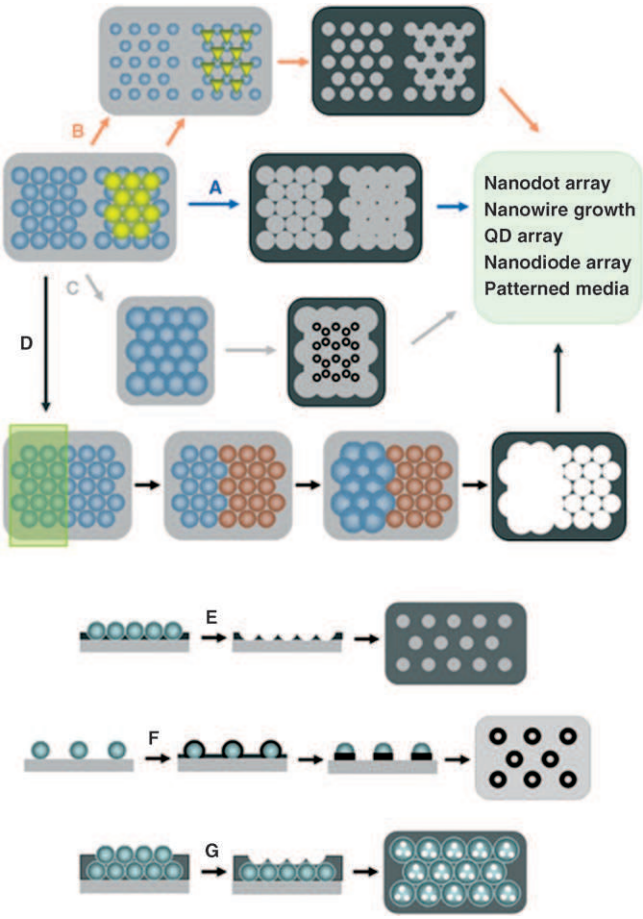

Figure 2. Typical nanofabrication routes of CL. Route A illustrates the simplest nanodot formation by depositing metal through an as-prepared colloidal mask. Routes B and C show the modification of a mask via RIE and annealing of the colloids in combination with a tilted-angle deposition. Route D is a scheme for hierarchical patterns using a photocurable colloid. Routes E and F are examples of a colloid used as a template for nanopattern formation: Route E shows a templating of organic and inorganic materials with a hexagonally packed structure, while route F shows the creation of nanorings using metal sputtering and ion milling. Route G shows the nanomachining process to fabricate regular holes on colloids for functionalization.

Meanwhile, self-assembled colloid arrays have been employed not only as masks but also as scaffolds for templating 2D or 3D functional patterns. For example, a honeycomb-structured functional material has been fabricated either by depositing a colloid containing the functional material or by post-deposition through the preformed colloidal mask, as shown in Route E of Figure 2. In most cases of CL, colloid arrays are used as masks or scaffolds for the deposition or etching of some specific materials. For example, a simple method is available for fabricating metallic nanoring arrays by ion milling a deposited metal on the colloid surface, as shown in Route F of Figure 2, or the colloidal particle itself can be functionalized by employing suitable lithographic techniques (Route G of Figure 2). The patterned particles can be functionalized further via nanomachining or by selective deposition of a functional material into the patterned holes of the particles. In the subsequent sections, we will review the current CL techniques that use colloidal crystal layers as masks or as functional composite materials, focusing on the various methods for fabricating nanoscopic patterns.

3.1. Nanopatterning with Colloidal Masks

3.1.1. Direct Deposition or Etching using Colloidal Masks

The use of a self-assembled colloid layer as a lithographic mask simplifies the mask fabrication process, which is one of the critical and time-consuming steps in conventional photolithography, requiring the exposure and development of a photoresist. Colloidal particles with a hexagonally packed array can be used as a mask so that deposition or etching proceeds through the interstices between the colloidal particles; a nanoscopic array of triangular metal dots can be obtained by direct deposition of the metal using a sputtering instrument such as a magnetron sputter, e-beam, or a thermal evaporator. The sputtered materials can be chosen without any limitations and the size, height, and number density of the metal dots can be controlled by simply adjusting the particle size and the sputtering conditions. In general, the use of interstices for deposition or etching can facilitate the formation of small-feature-size dot

 © 2006 Wiley-VCH Verlag GmbH & Co. KGaA, D-69451 Weinheim

arrays compared to the size of the colloidal particles. Therefore, most approaches have utilized the interstices between the particles to fabricate nanoscopic patterns in the early stages of fabrication.

More than twenty years ago, pioneering works in CL were conducted by Fischer et al. and Deckman et al. using colloidal particle arrays as masks for metal sputtering or etching of a substrate.[44] Since then, CL has attracted great attention, and recently the group of van Duyne has improved CL greatly.[45] As a mask for metal deposition, van Duyne and co-workers spin-cast single- or double-layered colloidal PS latex bead arrays on various substrates, as illustrated in Route A of Figure 2. The resulting pattern of the metals varied with the stacking structure of the colloidal array. Specifically, a hexagonally ordered triangular array of metal dots was formed from the single-layered colloidal mask, and a spherical dot array with different unit lattices was fabricated from the double-layered mask. The resulting patterns of the nanodot arrays are shown in Figure 3a and b.

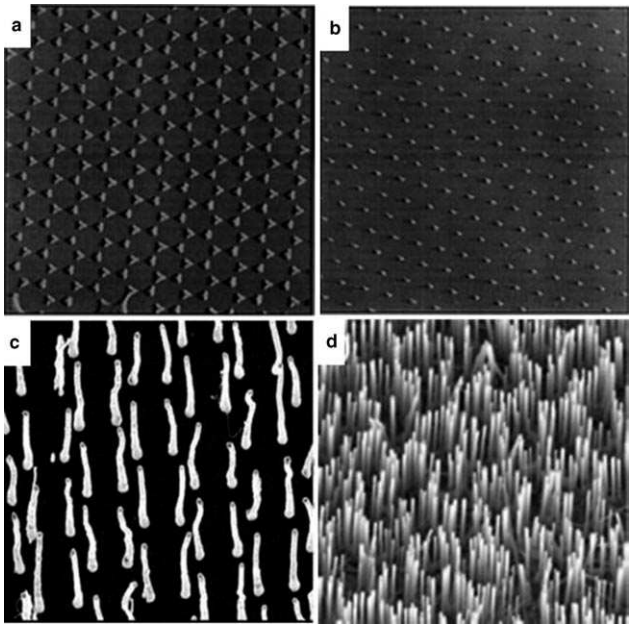

Figure 3. Metal-dot arrays formed by nanosphere lithography and the use of the nanodots as a seed material for the growth of nanotubes and nanorods: a, b) Nanodot arrays formed from single- and double-layered colloids, respectively. Metal dots were sputtered through the interstices among the self-assembled colloids. Reprinted with permission.[45] c) Vertically aligned carbon nanotube array. Reprinted with permission.[46] d) ZnO nanorods grown from seed materials deposited by nanosphere lithography. Reprinted with permission.[48]

Due to its flexibility and simplicity, the CL process has been applied for the nanofabrication of various organic and inorganic materials. In some cases, the deposited materials can be used as seeds for the growth of other functional materials; for example, carbon nanotubes were grown on nickel nanodots that were pre-deposited through a colloidal mask, as shown in Figure 3c.[46] In this work, a hot-filament plasma-enhanced chemical vapor deposition (PECVD) technique was employed to grow vertically aligned nanotube arrays.[47] CL-assisted nanorod growth was demonstrated also by Wang et al. using a Au array as a seed for a zinc oxide nanorod array, as shown in Figure 3d.[48] Pacifico et al. also proposed a method for fabricating a hexagonally arranged quantum dot array by modifying a deposited triangular array of silver.[49] Similarly, a discrete organic light-emitting nanodiode (OLED) array has been fabricated by CL-assisted patterning.[50] Generally, the patterning of OLEDs with a conventional masking process may not be feasible because an etching process can damage the organic heterostructures of the OLED layers. However, multilayer deposition of OLEDs through the interstices of the particle array was realized without causing etching damage, and the sub-100 nm pixellated OLEDs showed electroluminescence comparable with macroscale OLEDs.

Likewise, sputtered metal arrays can be used as etching masks to create surface topography. Kuo et al. demonstrated the fabrication of silicon nanopillar arrays with diameters as small as 40 nm and aspect ratios as high as seven.[51] The size and shape of the nanopillars can be controlled by the size and shape of the sputtered aluminum mask, which are again determined by the feature size of the colloidal mask and the number of the colloid layers. Nanopillars with different shapes can also be fabricated by adjusting the RIE conditions such as the gas species, bias voltage, and exposure duration for an aluminum mask with a given shape. As-prepared nanopillar arrays were utilized for imprinting a layer of PMMA above its glass transition temperature.[52] Utilizing a similar approach, Weekes et al. proposed the fabrication of a cobalt nanodot array for patterned magnetic media.[53]

CL is also suitable for modifying surface properties, which is useful for emerging applications in biotechnology. Patterns of chemical contrast often provide an efficient tool to investigate the interfacial interactions or adsorption behavior of biomolecules and nanoparticles.[54] Chemical dissimilarity is usually accomplished by the selective chemisorption of SAM substances terminated with biocompatible moieties of carboxylic acids or amine groups. Chemically and structurally designed interactive sites for the attachment of target proteins in a modified surface with SAMs were demonstrated by Michel et al.[55] Chemical contrast was achieved by the adsorption of protein-friendly dodecyl phosphate (DDP) ions onto titanium oxide and protein-repellent polycationic poly-L-lysine grafted poly(ethylene glycol) onto silicon oxide. Further binding of streptavidin on DDP and immobilization of biotinylated liposomes to the streptavidin was accomplished successfully. Also, a bimetallic pattern, composed of gold and titanium oxide as a valley and mesa (or vice versa) was created by sputtering on a particle layered surface.[56]

Although polymer particles cannot sustain their structures under exposure to oxygen plasma, their ordered arrays can be used as masks for fabricating a dome structure. The reactive plasma can be dispersed by the particle in a point-contact with a substrate, which induces the so-called underetching of the colloidal mask and eventually produces a dome structure of the substrate. Underetching can be avoid-

 © 2006 Wiley-VCH Verlag GmbH & Co. KGaA, D-69451 Weinheim

ed by modifying the shape, size, and coverage of the colloidal mask, which will be discussed later. Tan et al. demonstrated the characteristic features of a reactive-ion-etched silicon substrate using a PS mask and produced a double dome structure by simultaneous etching of the mask and the regions beneath the particles.[57] Constituting another advantage of CL, the colloidal mask can be removed only by sonication, without causing any damage to the polymeric substrate, which is a favorable feature compared to the development or lift-off process in photolithography using organic developers. For example, polyacrylic acid (PAA) was patterned by oxygen plasma onto a self-assembled PS mask with almost no damage to the top of the polymeric dome structure, and a protein was then inked to the PAA surface.[58] Recently, Co/Pd magnetic multilayers were sputtered onto polymeric latex-sphere surfaces.[59,60] In this case, it is not necessary to lift off the particle template and etch away the substrate because magnetic domains can be isolated by the surface topography of colloidal arrays with no need for additional patterning.

Over the last decade, 3D colloidal crystals have been developed for macroporous structures of various substances including conducting and semiconducting polymers and magnetic materials.[61] Several techniques such as e-beam lithography, electrochemical etching, and microcontact printing[62] have been used for fabricating porous films. However, both the fabrication of very thin porous films with one-pore thickness and morphology control pose significant challenges to the aforementioned techniques. In the following summary, the patterning routes using colloidal monolayers for useful periodic structures including macroporous membranes and hemispherical shells are discussed.

Spherical colloidal particles can be utilized for fabricating arrays of macropores or shells by electrodeposition (ED) or atomic layer deposition (ALD) of a gold film.[63–67] In comparison to other deposition methods, these deposition processes proceed homogenously and yield a smooth surface with uniform thickness. In contrast to isotropic deposition methods such as ED and ALD, the sputtering of metals in a vacuum chamber facilitates the formation of metal shells on the exposed areas of the colloids due to the anisotropic features of directed sputtering. A metal dome and dot array can be formed by deposition of a metal onto colloidal particle surfaces.[68,69] The anisotropy of the sputtering method generally provides selective deposition on the particle surface. However, it is sometimes necessary to coat the entire surface of the colloids, except for the contact point at the substrate, via tilted and rotational deposition. Simple deposition onto the colloidal particle array and subsequent removal of the core particles produced crescent moons each with a sharp edge, which cannot be obtained with other methods. This unique structure was used for biomolecular detection by surface-enhanced Raman scattering (SERS).[70] Notably, the local electric field was amplified in the sharp edge of the crescent moon structure.

Complete deposition of a metal on the colloid particle array can also be utilized for fabricating high-density gold and cobalt ring arrays for optical and magnetic applications.[71,72] As an alternative method for producing ring structures, so-called edge-spreading lithography (ESL) using a close-packed colloid array has been proposed by McLellan et al.[73] ESL utilizes the surface diffusion of a substance forming a SAM. For ring formation, a monolayer of silica particles was self-organized on gold and silver surfaces and SAMs of an alkanethiol were formed on the substrate around the contact points of the silica spheres at the substrate. The SAMs of the alkanethiol around the contact points were used as masks protecting the underlying substrate during wet etching and eventually producing gold and silver ring arrays. The ESL method was also employed by Geissler et al. to fabricate multiple ring structures with alkanethiolates using a silica colloid, as shown in Figure 4.[74] This approach successively transferred three different SAMs onto a gold surface guided by the silica colloids, and a double concentric ring structure was obtained after wet etching.

Colloidal arrays have been used in imprinting processes for caved spherical morphologies. When hydraulic pressure was applied onto a particle array over an aluminum substrate, the protruding morphology of colloidal spheres leaves behind an ordered array of spherical indents on the substrate, which acts as seeds for nanopores on the aluminum surface during the anode etching process. The prepatterning of an aluminum film with ordered spherical indents improved the ordering of nanoholes in aluminum oxide.[75,76] Similarly, the morphology of a colloidal array was replicated into a polymer surface.[77,78]

3.1.2. Modification of Colloidal Masks

Although the preparation of a colloidal mask is facile and cost effective, the resulting pattern with a colloidal array is limited to triangular or spherical structures. In many applications, the material properties are highly dependent on the shape of the patterned species as well as the feature size, and patterning techniques to generate a variety of feature shapes are required. A few examples are localized-surface plasmon resonance (LSPR),[79] SERS,[80] and spin dynamics of magnetic metal dots.[81] In this regard, however, the limited controllability of the patterned shape of the materials is a distinct disadvantage of CL compared to other lithographic techniques. To overcome this disadvantage, two strategies have been suggested; namely, adjustment of the deposition method and modification of the colloidal masks.

Modification of the deposition scheme is generally achieved by a simple tilted or rotated deposition through as-prepared colloidal masks. The tilt angle is defined by the angle between the etchant (or deposition) flow and the normal to the substrate. By using this method, the sputtered shapes can be modified to elongated triangles or double triangles via a single deposition at a given tilted angle or a multiple deposition at different angles.[82] However, tilted deposition or etching has also limited tunability in the resulting patterns due to the intrinsic restrictions of the mask shape.

A more effective approach is to modify the colloidal particle from spherical to another shape by employing a suitable post-treatment of a self-assembled spherical colloi-

 © 2006 Wiley-VCH Verlag GmbH & Co. KGaA, D-69451 Weinheim

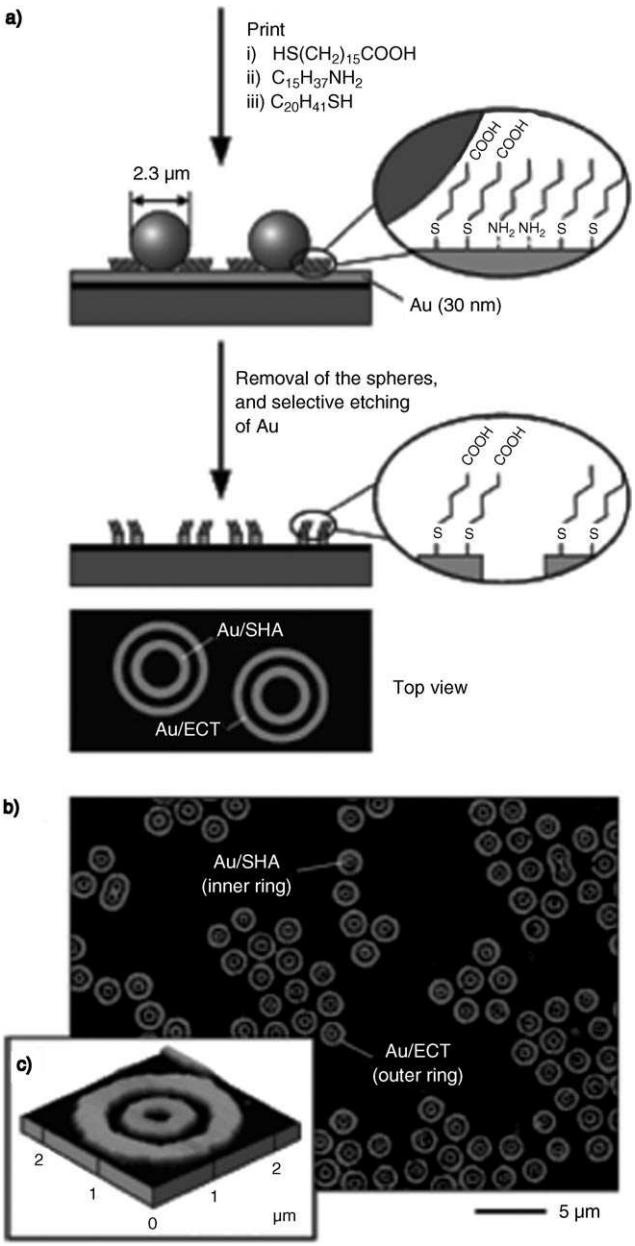

Figure 4. Fabrication scheme for concentric gold rings using ESL: a) Multiple deposition of self-assembled monolayers (SAMs) on a gold substrate by spreading SAMs on the silica colloids. Three different SAMs were spread consecutively by printing on the colloid layer. After the removal of colloidal spheres, both the unprotected Au layer and the area covered by the alkylamine SAMs were etched away. b, c) SEM and AFM images of the concentric gold rings. The gap between the two rings is 250 nm. The widths of the inner and outer rings are 260 and 340 nm, respectively. Reproduced from Ref. [74].

dal array. In particular, RIE, ion milling, or annealing provides a versatile means for fabricating nanoscopic patterns of novel features, which cannot otherwise be obtained by conventional lithographic techniques.

In general, polymers are composed mainly of carbon chains, and show a glass transition above a certain temperature (T_g) due to the free-volume change between the polymer chains.[83] Polymeric particles such as PS and PMMA latexes also exhibit a glass transition at elevated temperatures. Therefore, the deformation of spherical polymeric beads above T_g has been utilized to modify the colloidal mask for fabricating a gold disk array via CL.[84] In doing this, the size of the disc was controlled by adjusting the degree of annealing, because the polymeric particles spread over a wider distance with the annealing time. Similarly, annealing the polymer particles can also be achieved by microwave heating of the substrate.[85] By adjusting the intensity of the microwave radiation, the degree of annealing can be controlled more precisely than with thermal heating in an oven. Figure 5a illustrates the progressive deformation of polymer particles

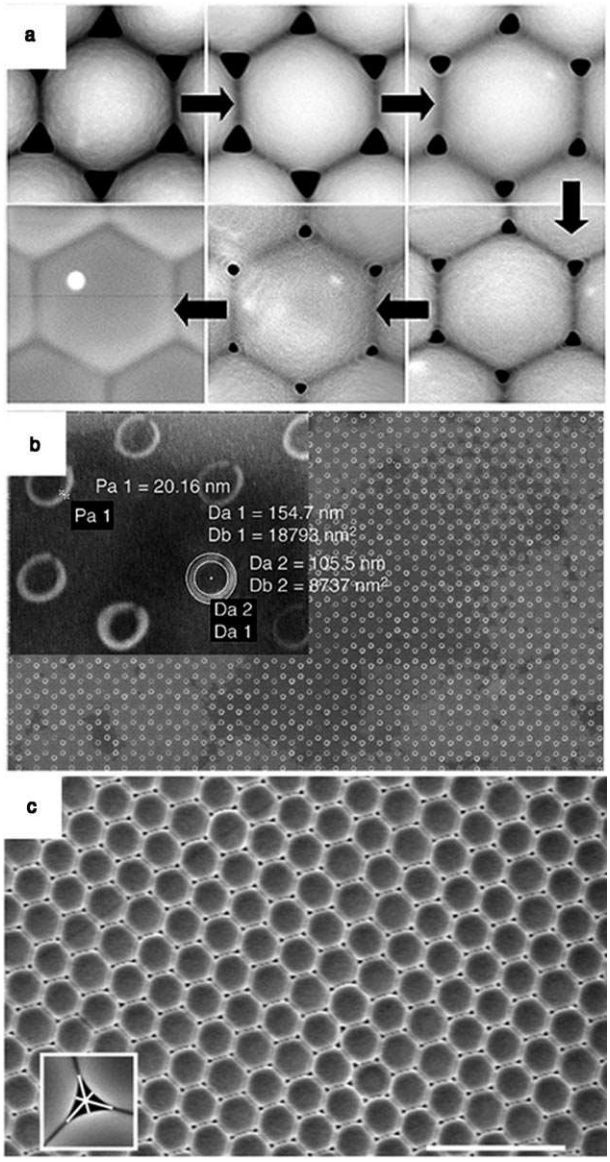

Figure 5. Modification of a colloidal mask by deforming the colloid array: a) Precise control of the degree of annealing is achieved via adjustment of the number of microwave exposures; the size of the interstices was controlled by the degree of annealing. b) Nanoring structure fabricated by rotational tilted deposition through the annealed colloidal mask shown in (a). Reproduced from Ref. [85]. c) Silica colloid deformed by ion bombardment. Reprinted with permission.[86]

 © 2006 Wiley-VCH Verlag GmbH & Co. KGaA, D-69451 Weinheim

with increasing microwave pulses. Rotated deposition at a tilted angle with an annealed mask provides a number of unique patterns such as ring arrays, as shown in Figure 5b. In addition, the modification of inorganic masks can also be achieved by plastic deformation using ion irradiation (Figure 5c).[86] Silica particles were deformed by ion bombardment and expanded in the plane perpendicular to the ion beam.

Meanwhile, RIE provides a versatile tool for the modification of a colloidal mask by changing the size and shape of the constituent colloidal particles.[87] RIE has been usually employed to control surface morphology and roughness and to enhance surface hydrophilicity in biological applications.[88] Recently, we fabricated well-organized layers of nonspherical colloidal particles through the use of anisotropic RIE onto multilayered spherical PS latexes, in which the top layer acted as a shadow mask.[89] The resulting patterns and particle shapes were dependent on the crystal orientation relative to the substrate, the number of colloidal layers, and the RIE conditions (Figure 6). The shadowing effect from the upper-layer particles to the layers beneath results in nonspherically etched polymeric structures. The shape of the resulting colloidal pattern varied dramatically according to the stacking sequence of the colloidal crystals. In addition, crystal orientation relative to the etchant flow affects the structure of the resulting colloidal pattern. Colloidal spheres can produce fcc and hcp crystal structures, which differ in the stacking of the hexagonally close-packed (111) layers. Usually, the (111) planes are parallel to the substrate surface when the colloidal layers grow free from a geometrical confinement. However, colloidal layers can be grown with the (100) plane facing the etchant flow by introducing microchannels, V-shaped grooves, and pyramid pits, which act as confined geometries.[90] An approach by Choi et al. constitutes a new way for creating colloidal masks with polygonal structures that cannot otherwise be produced by CL alone.[91] With a polygonal mask, arrays of circular dots and holes as well as triangular dots of multilayered magnetic metals were prepared. Further optimization of the experimental conditions and combination with other lithographic tools are expected to yield other novel patterns at the nanometer scale.

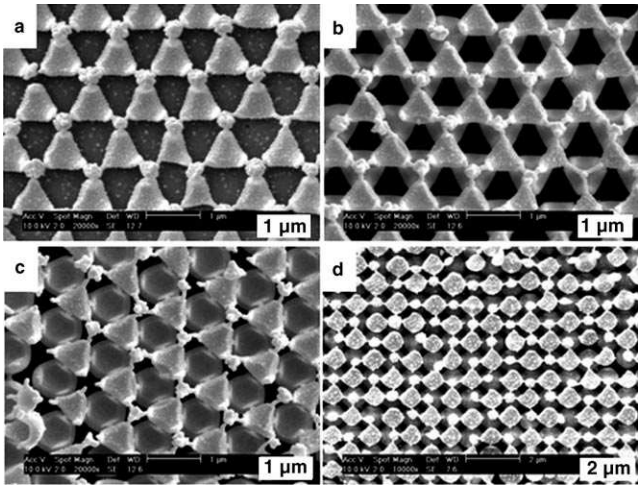

Figure 6. Modification of a mask using RIE for the fabrication of binary and ternary particle arrays with nonspherical building blocks. a, b) Triangle arrays using binary and ternary colloidal spheres with an hcp arrangement. c, d) Polygonal structures produced from colloidal layers with the (111) plane and the (100) plane of the fcc structure, respectively. Reprinted with permission.[89]

CL can be used with a 2D array of particles as a shadow mask or with the interstices between particles as open windows for reactive ions to create patterned bumps or pores on a substrate. Indeed, CL allows considerable freedom to control both the feature dimensions and shape of nanopores by changing the particle size and the stacking sequence of multilayered particle arrays or by using angle-resolved etching. Although recent advances in CL readily allow the formation of bulk patterns with nanoscopic features, the structural hierarchies are an essential step toward the practical applications of these substrates.

Recently, our group demonstrated a photolithographic process to produce hierarchical arrays of nanopores or nanobowls with colloidal photoresist particles.[92] Emulsion copolymerization of styrene or methylmethacrylate (MMA) with glycidyl methacrylate (GMA) was used to synthesize submicrometer-sized photoresist particles of poly(styrene-*co*-glycidyl methacrylate) (PSGMA) or poly(MMA-*co*-GMA). Then, these copolymer particles could be crosslinked with themselves under UV-exposure with no need for crosslinking monomers in the colloidal medium. Figure 7A–C shows the overall CL process for the hierarchical patterning of nanopore arrays on a silicon substrate with crosslinked PSGMA particles.[92a] First, PSGMA photoresist particles with a photoinitiator were deposited onto a silicon substrate and self-organized into a 2D array on a silicon substrate. Then, by using a photolithographic process (UV exposure and post-exposure baking) with designed masks, localized domains of the photoresist particle array were crosslinked selectively with micrometer-scale periodicity (Figure 7A). The large difference in T_g between crosslinked (UV-exposed) and non-crosslinked (UV-screened) particles was the most favorable factor to produce a high contrast in interstitial pore sizes during baking. Therefore, when baked at a temperature above T_g of non-crosslinked PSGMA but below T_g of crosslinked PSGMA, the unexposed particles were deformed but the exposed part of the particle array retained its structure (Figure 7B). Finally, the patterned colloidal particle arrays were used as masks for RIE. Etching proceeded only in the previously UV-exposed region and produced a patterned array of nanopores on the substrate (Figure 7C). SEM images of the products from the processes described above are given in Figure 7a–d. These 2D porous substrates have attracted great attention for a wide range of applications including chemical microcontainers, surface-plasmon resonance biosensors, catalytic supports, and photonic crystals.

Our group have also reported the same photolithography-assisted CL with photoresist particles of poly(MMA-*co*-GMA) to produce multiscale patterns of nanobowl arrays.[92b] The overall strategy is depicted in Figure 8A–D.

 © 2006 Wiley-VCH Verlag GmbH & Co. KGaA, D-69451 Weinheim

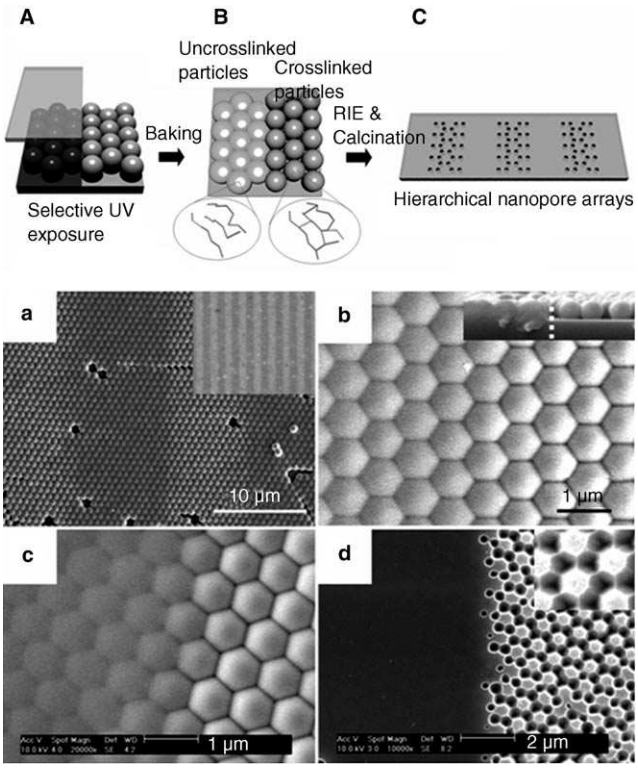

Figure 7. A–C) Schematic of the photolithographic patterning of 2D colloidal crystals and hierarchical colloidal lithographic patterning of a substrate. a–d) SEM and optical microscope images of the patterned structures. a) SEM image of a patterned two-dimensional colloidal crystal (inset: optical microscope image of the patterned colloidal crystal). b, c) Magnified SEM images after post-exposure baking for 5 min and 7 min, respectively (inset in (b): cross-sectional SEM image around the boundary between the exposed and unexposed parts of the colloidal array). d) SEM image of a silicon substrate that was nanobored by colloidal lithography using a prepatterned colloidal crystal (inset: magnified image of the pore arrangement). Reproduced with permission.[92a]

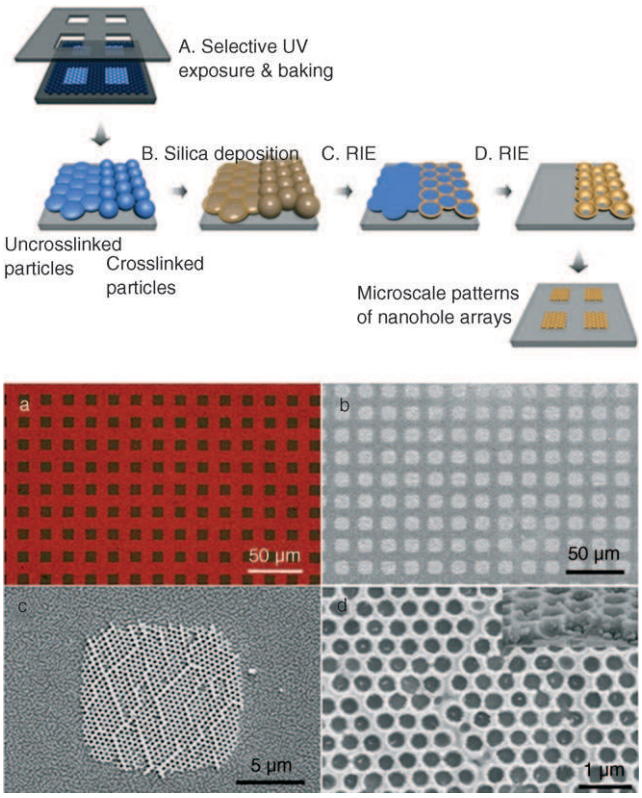

Figure 8. A–D) Schematic diagram of colloidal lithography using photoresist particles. a–d) SEM and optical microscope images of the patterned structures: a) Optical microscope image of a gold-coated patterned nanohole array fabricated by colloidal lithography and subsequent silica deposition. b) SEM image of patterned nanohole arrays. c) SEM image of a single domain of a nanohole array. d) Magnified SEM image of a single domain of a nanohole array (inset: cross-sectional view of the nanohole array). Reproduced from Ref. [92b].

First, the photoresist particles were deposited onto a silicon substrate and exposed to UV radiation through a mask. Then, subsequent annealing of the photoresist particles modulated the size of the interstitial pores between the particles (Figure 8A). These procedures created a colloidal mask with domains of ordered interstitial nanopores patterned on a micrometer feature scale. Finally, chemical vapor deposition through the colloidal mask and subsequent etching produced a hierarchically organized inverted nanobowl array on the silicon substrate. (Figure 8B–D). The resulting optical microscope and SEM images of a large area of patterned silica nanobowl arrays are shown in Figure 8a–d. As noted, the nanobowls were arranged into well-ordered hexagonal symmetry.

3.2. Nanolithography for Functional Multifaceted Particle Arrays

Recently, a new nanolithography strategy for the fabrication of arrayed colloidal particles, each with nanopores in threefold or fourfold symmetry, was developed.[93] This was the first report on the fabrication of monodisperse particles with regularly patterned nanoholes by CL. A scheme of the nanolithography used is shown in Figure 9. First, a self-organized double layer of PS microspheres was dip-cast and the interstices between the PS microspheres were filled with silica nanoparticles above the bottom layer but below the top layer. Partial RIE was then used to remove the top-layer PS microspheres leaving behind an ordered monolayer of macropores in silica matrix each with windows connected to the bottom layer of PS microspheres (Figure 9c). This silica matrix with regularly patterned windows was then used as a colloidal mask for further RIE processing. As a result, the PS microspheres of the bottom layer were sculptured and possessed nanoholes, as shown in Figure 9d.[93] The resulting SEM images of the PS microsphere arrays are shown in Figure 10a and b. The nanopores are arranged in threefold or fourfold symmetry depending on the stacking sequences of the PS microspheres. The threefold symmetry was created when the (111) plane of the PS microsphere packing was exposed to the RIE etchant flow whereas the fourfold symmetry originated from the situation where the (100) plane was facing the etchant flow.

 © 2006 Wiley-VCH Verlag GmbH & Co. KGaA, D-69451 Weinheim

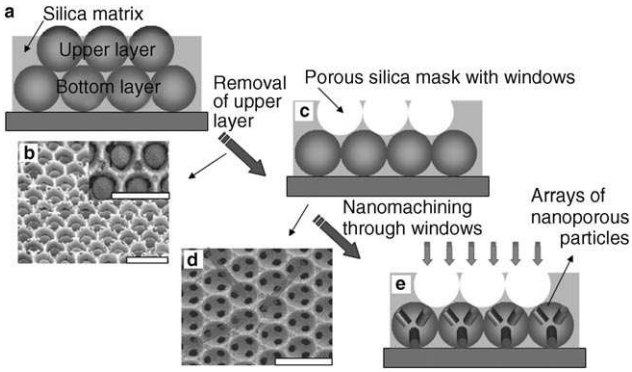

Figure 9. Nanomachining for the fabrication of an array of colloidal particles with patterned pores by using colloidal masks: a, b) Schematic of a colloidal double layer of polymer beads embedded in silica matrix and the corresponding SEM image, respectively, in the nanomachining procedures. c) Porous silica mask with windows, which is formed after removal of the top layer of polymer beads. d, e) Using a silica mask for the subsequent RIE process in which the polymer beads of the bottom layer can be sculptured according to the shape of silica window (scale bar is 2 μm). Reprinted with permission.[93]

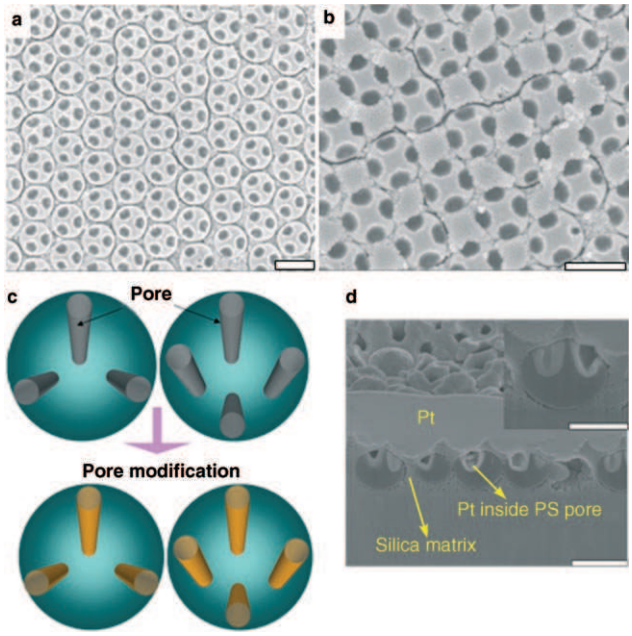

Figure 10. a) Planar SEM image of PS particles with patterned pores of threefold symmetry where the (111) plane was directed toward the etchant flow in RIE. b) Planar SEM image of PS particles with patterned pores of fourfold symmetry where the (100) plane was parallel to the substrate and directed toward the etchant flow in RIE. c) Schematic of the fabrication of composite PS particles with regular pores. d) Cross-sectional SEM image of Pt incorporated into composite particles where the (111) plane of the fcc structure of the colloidal layer was facing the sputtering flow (scale bars are 1 μm). Reprinted with permission.[93]

These patterned particles with regular holes produced by nanolithography using colloidal self-assembly and RIE can be applied to the fabrication of functional composite particles. A variety of organic and inorganic materials such as metals for metal–polymer composites, DNA and proteins for biological applications, semiconducting and ceramic materials, and other polymers and small chemicals for drug delivery can be incorporated via chemical and physical attachments, as illustrated in Figure 9e and Figure 10c. To demonstrate the process, Pt-incorporated PS–Pt composite particles were fabricated using ion sputtering, as shown in Figure 10d.[93]

Recently, our group extended previous work to demonstrate the fabrication of microparticles with controlled shapes by colloidal lithographic sculpturing of microsphere arrays.[94] Three different systems were used to achieve this; namely, multilayered PS microspheres, composite films of PS microspheres and silica nanoparticles, and binary colloidal layers of PS and silica microspheres with comparable size ratios. In CL with reactive ion etching, the upper layer acts as a mask for the lower layers by a relative shadowing effect. Consequently, the resulting morphologies of the sculptured PS microspheres were largely dependent on the crystal orientation relative to the etchant flow, the number of colloidal layers, the size ratio of silica to PS microspheres, the etching angle in the RIE process, and the stacking sequence of the binary colloidal layers. Figure 11a and c shows schematics of anisotropic RIE of double-layered PS microspheres with different tilt angles, and the resulting SEM images of the sculptured PS microspheres are reproduced in Figure 11b and d, respectively. Indeed, the resulting shapes of the sculptured PS microspheres in the bottom layer changed dramatically with the tilt angles (θ) of the substrate and the orientation angle of the crystal plane, both relative to the etchant flow in the RIE process. Specifically, PS microparticles with one large lump and two small lumps were obtained (as shown in Figure 11d) because of a relative shadowing effect. If the layered colloidal crystal was rotated by 60° (or 180°) around the axis normal to the substrate and subsequently exposed to the RIE process, a different structure having two large lumps and one very small lump could be also obtained as a result of the altered shadowing effect. This method can be extended to a triple-layered colloidal crystal.

A novel composite structure patterned with sculptured PS particles embedded in a silica matrix could be obtained by using a mixed suspension of PS microspheres and silica nanoparticles, as shown schematically in Figure 11e and g. As noted from the SEM images in Figure 11f and h, the shape of the sculptured PS particles is dependent on the thickness of the silica matrix as well as the tilt angle. In addition, the depth of the pores inside the PS particles can be controlled by the length of the RIE process. PS particles with anisotropic holes of different depths were obtained by a tilted RIE process using a silica mask with windows of threefold or fourfold symmetry. For example, tilted RIE produced the PS microparticles with two large holes and a shallow one on the surface of the microsphere, as shown in Figure 11h. The number of windows open to an underlying PS microsphere is dependent on the orientation of the colloidal stacking.[94] Using these silica masks with different window configurations, arrays of nanobored particles with

 © 2006 Wiley-VCH Verlag GmbH & Co. KGaA, D-69451 Weinheim

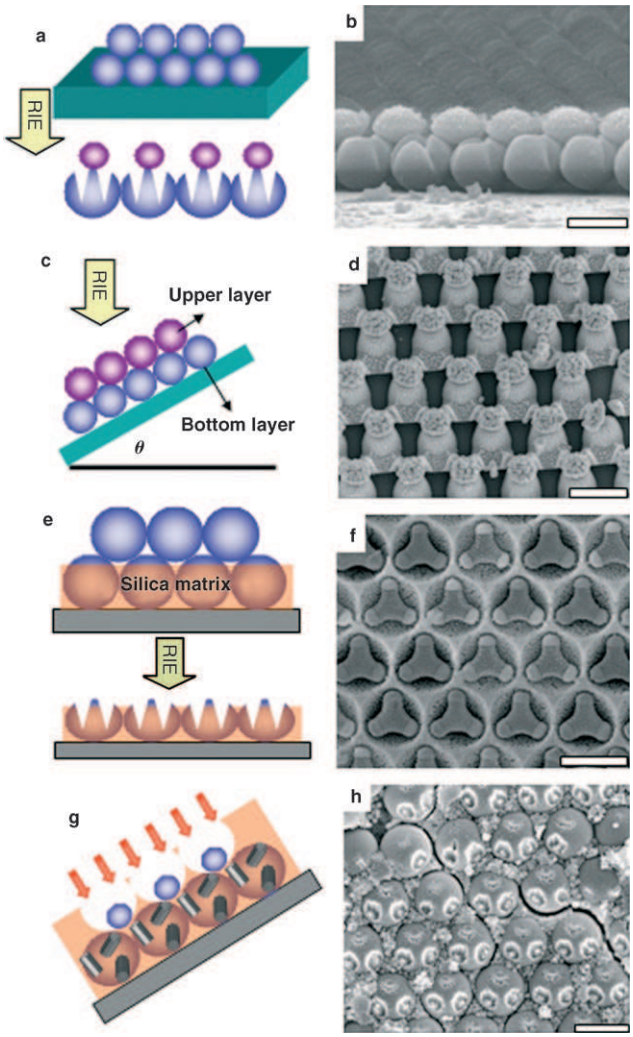

Figure 11. a, b) Schematic of the planar RIE process and a cross-sectional SEM image of sculptured PS particles using double-layered colloidal PS beads of 1.01 μm in diameter, respectively. c, d) Schematic of a tilted RIE process and the resulting SEM image of sculptured PS particles using double-layered PS beads, respectively. The tilt angle, θ, was 30°. e, f) Schematic of the sculpturing process and the resulting SEM image of sculptured PS particles using double-layered PS beads of 1.01 μm diameter formed in a silica matrix. The silica nanoparticles were 50 nm in diameter. g, h) Schematic of the fabrication of PS beads with anisotropic holes of different depths and the resulting SEM image of a hexagonal PS bead array with three anisotropic holes of different depths after removal of the mask with adhesive tape. Scale bars represent 1 μm. Reproduced from Ref. [94].

three or four anisotropic holes can be produced in a controllable manner.

Likewise, this strategy of nanosculpturing colloidal particles can be extended to binary colloids self-organized by layer-by-layer growth.[94] As an illustrative purpose, two different spheres of silica and PS of comparable size were used. Silica spheres with various sizes were self-assembled onto a preformed monolayer of PS microspheres. Inorganic silica spheres played the role of a mask against the oxygen RIE in a direct nanosculpturing of the underlying hexagonally packed PS microspheres. This procedure sculptured a number of interesting patterns on the PS particles, which cannot be easily produced by conventional lithographic techniques. The oxygen plasma penetrated through the interstices of the silica spheres and etched the surfaces of the PS microspheres. Depending upon the RIE conditions, the stacking structure and the size ratio of silica to PS microspheres, the surface morphology of polystyrene varied dramatically after removal of the silica microspheres using HF. The resulting SEM images are reproduced in Figure 12.

4. Applications of CL-Assisted Nanopatterns

Thus far, CL-assisted nanofabrication has created new types of nanopatterns. As has been previously shown, CL can readily create nanoscopic polygonal metal dots with sharp edges, which are not available through conventional lithography. These patterned materials display structure-dependent optical or magnetic responses. Although e-beam lithography has sub-30 nm resolution, it is not facile to fabricate sharp edges at this resolution due to the beam spot size. Also, conventional lithography is not able to fabricate hollow cylinders with sub-100 nm diameter and wall thickness. Therefore, research on CL has focused on the fabrication of nanostructures that have not been available with conventional lithography. In this section, we review the applications of CL-assisted nanopatterns, emphasizing optical, biological, and magnetic media applications, which utilize the shape-dependent properties.

Metal nanopatterns have attracted considerable interest because of their potential applications in bioanalytical chemistry, bioseparation, bioimaging, magnetism, ultrahigh density recording media, and others.[95] In particular, gold-nanoparticle-induced LSPR can be applied in biological, optical, and photonic devices.[96] LSPR utilizes the collective oscillation of conduction-band electrons that arises in a metal nanopattern under excitation by a specific wavelength of electromagnetic radiation. Generally, the resonance induces strong absorption or scattering of the incident light and a local electric-field enhancement. The position of maximum extinction (λ_{max}) and the peak shape are related to the shape, size, and composition of the nanopatterned domains, the feature distance, as well as the external dielectric environment. The extinction spectra of the nanopattern exhibits measurable wavelength shifts that correspond to small changes in the refractive index within the electromagnetic fields surrounding the nanopattern. In order to investigate the electromagnetic interactions, van Duyne and co-workers have studied shape dependence and domain–domain interactions of the metal nanopatterns by measuring the LSPR of hexagonal,[97] square, or linear arrays[98] of Au and Ag cylinders, which were prepared by e-beam lithography. The experimentally observed changes in the peak shape and position of LSPR were compared with theoretical calculations by Kelly et al.[99] Despite the high accuracy of e-beam lithography, this approach is not attractive due to its high cost. Consequently, a more simple lithographic tool based on self-assembly has been required and CL is one of the potential candidates.

 © 2006 Wiley-VCH Verlag GmbH & Co. KGaA, D-69451 Weinheim

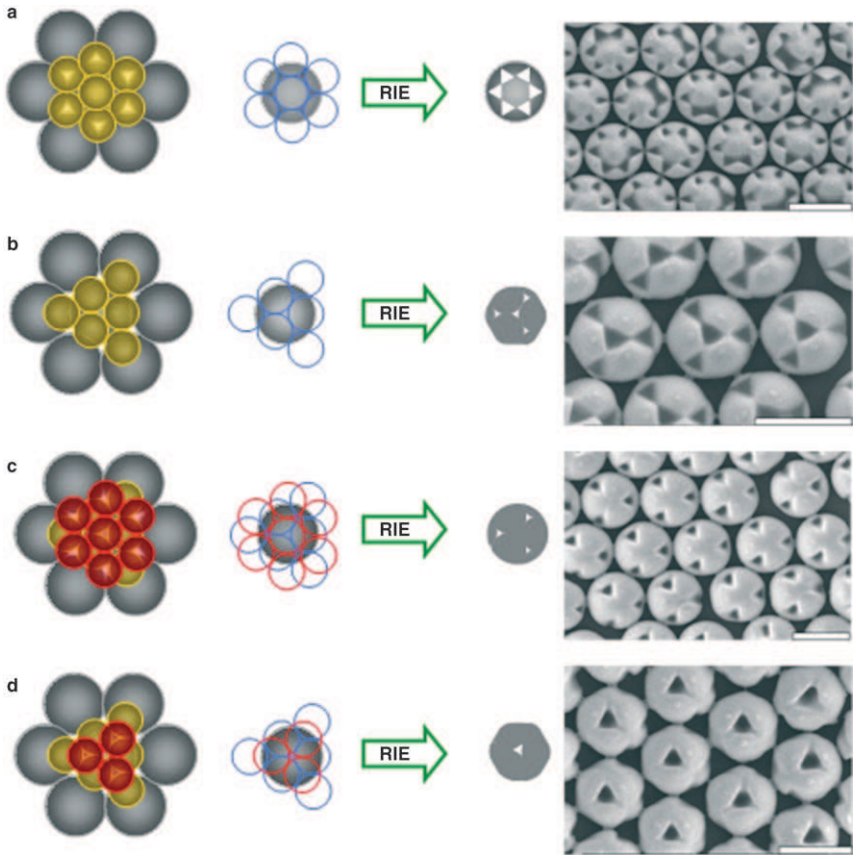

Figure 12. Schematic of binary colloidal stacking sequences and the resulting SEM images of sculptured PS beads produced by oxygen RIE. SiO_2 spheres were coated onto the preformed monolayer of spherical PS beads. The SEM images of the PS spheres after RIE and removal of the SiO_2 layers with HF are reproduced on the right-hand side of the Figure. a–d) Schematics of binary colloidal stacking sequences for a fixed size ratio at 0.574. The diameter of the PS spheres and scale bars are 1.01 μm and 1 μm, respectively. Reproduced from Ref. [94].

For shape-dependent optical properties, gold rings[71] and disks[84] were prepared using CL. In these experiments, CL was able to vary the feature sizes and shapes of the rings and disks in a controllable manner. In particular, tunable LSPR was achieved by varying either the diameter of the disks at a constant disk height or the ring thickness, as shown in Figure 13. It can be seen from the extinction spectra that as the wall thickness of the nanorings decreased the extinction peak was red-shifted. The shape-dependent red shift originates from the electromagnetic coupling between the inner and outer ring surfaces, which leads to energy shifts and splitting of degenerate modes.[100] In addition, CL was used for the fabrication of nanocaps and nanocups, which exhibited the optical extinction.[101] The nanocaps and nanocups were fabricated through the deposition of metal on the particle surface and subsequent removal of the colloidal particles.

One of the most promising applications of metal nanopatterns is in the preparation of biosensors or chemosensors for the detection of biological species and the diagnosis of disease. Recently, Haes et al. reported a detection method involving a biomarker for Alzheimer's disease using the LSPR of a nanopattern array fabricated by CL.[102] Their results demonstrate that a CL-derived pattern can be designed for the optimal analysis of complex biological species detecting the variation of extinction peaks in response to the attachment of guest molecules. In this work, the interaction between antigens and amyloid-β-derived diffusible ligand (ADDL) antibodies was studied using a sandwich assay. In addition, the proportionality between the concentration and the degree of peak shift of LSPR determined the ADDL concentration. When antibody-functionalized nanodots were exposed to the cerebrospinal fluid (CSF) of an aging patient or an Alzheimer's disease patient, a significant LSPR shift was detected.

Meanwhile, SERS is also a useful detection tool for bio- or chemical sensing devices.[80b] The SERS measurement is a spectroscopic technique that combines laser spectroscopy with the exciting optical properties of metal nanostructures; a strong increase of Raman signals occurs when molecules are attached to a noble-metal nanopattern. Since SERS takes place in the local fields of a metal nanopattern, the lateral resolution is determined by the confinement of the local fields, which can be two orders of magnitude higher than the diffraction limit. SERS is characterized by an ensemble-averaged intensity enhancement factor for analysis of the binding to noble-metal surfaces with sub-100 nm feature sizes.[103] In addition, SERS offers a high structural selectivity and sensitivity for extremely small volumes and enables single-molecule detection in DNA sequencing.[104] Recently, a few studies have been conducted on SERS behavior using CL-derived nanostructures. For example, Lu et al. generated strong Raman enhancement from a gold crescent moon structure with a sub-10 nm sharp edge.[70] As shown in Figure 14a, the emitted field on the circular sharp edge of the nanocrescent moon (named the "hot spot") can be enhanced by a factor of over one thousand under illumination at 785 nm from a near-IR diode laser. Interestingly, 1 μM of rhodamine 6G molecules adsorbed on the single gold nanocrescent moon could be detected with recognizable difference in the SERS spectrum, as illustrated in Figure 14b. This high sensitivity is due to the sharp edge of the nanostructure created from the colloidal template.

Recently, CL has been used to pattern proteins or cells for biosensors, bioreactors, and tissue engineering.[105] Generally, protein adsorption has been controlled by chemical contrast using selective binding or repelling of proteins. Denis et al. fabricated a patterned surface composed of gold and titanium oxide using CL, and demonstrated the poten-

 © 2006 Wiley-VCH Verlag GmbH & Co. KGaA, D-69451 Weinheim

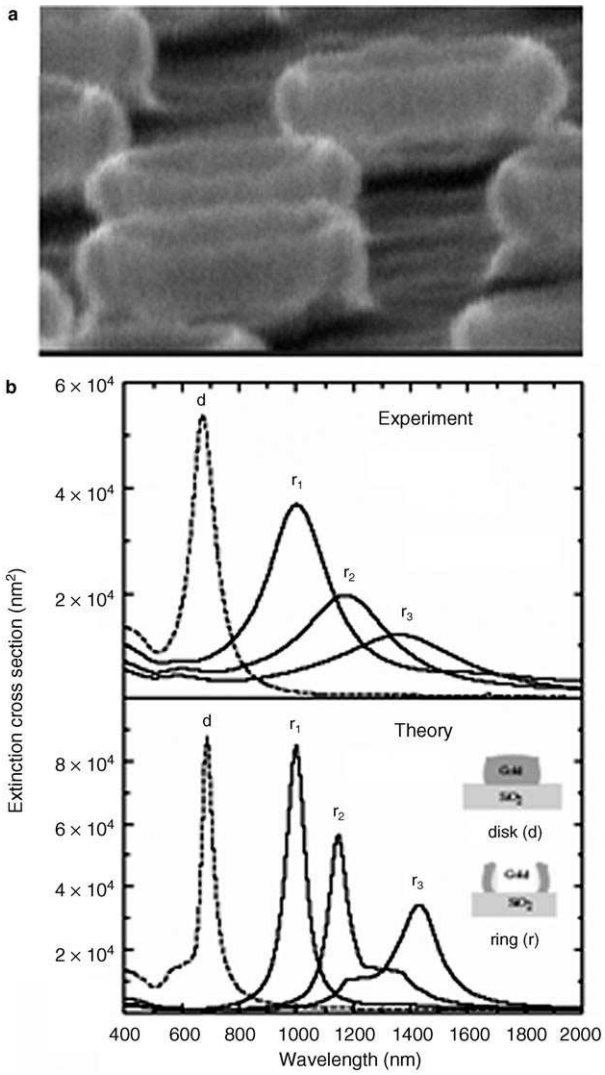

Figure 13. a) Side-view SEM image of gold nanorings. The thickness of the ring walls was estimated to about 14 nm. b) Experimental and theoretical extinction spectra of gold disks and rings. The maximum peaks are red-shifted by reducing the ring thickness. Reproduced with permission.[71]

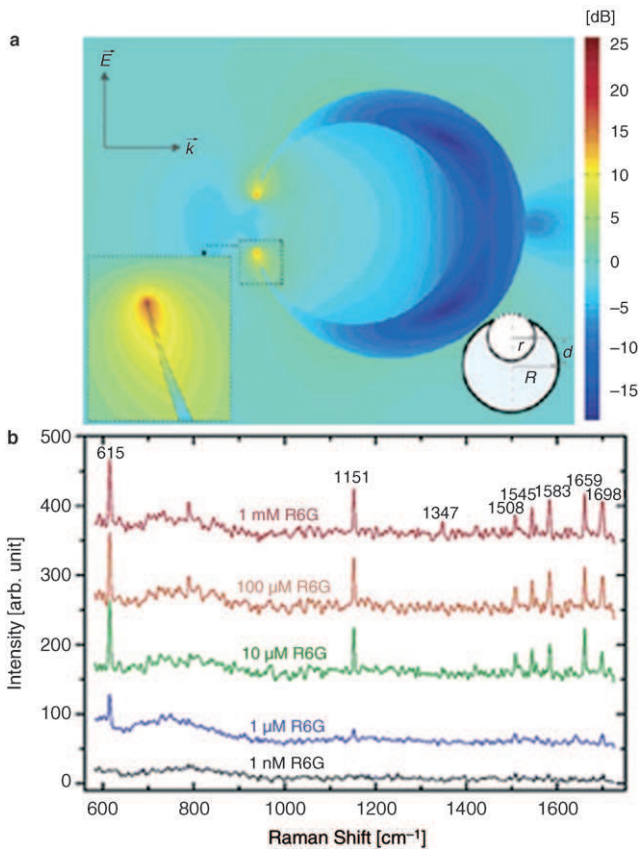

Figure 14. Nanoscale crescent moon structure for biomolecular detection fabricated from a colloid template: a) Simulated local-electric-field amplitude distribution of a nanocrescent moon at one of its scattering peak wavelengths (785 nm). b) SERS spectra of rhodamine 6G (RG6) molecules adsorbed on a "hot spot" of a single crescent. R6G molecules on the crescent moon could be detected at concentrations as low as 1 μM. Reprinted with permission.[70]

tial use of a heterogeneous pattern as a template for the selective adsorption of biomolecules by modification of the surfaces with suitable SAMs.[56] Similarly, Michel et al. fabricated a patterned array of biotinylated liposomes using selective binding of dodecyl phosphate to titanium oxide.[55] In these patterning procedures, however, nonspecific binding can occur during the multistep binding of biomolecules. In order to reduce the nonspecific binding of the protein array, Wang and Zhang developed the micropatterning of colloids, which were covered by proteins on the surface.[106] Because colloids covered with proteins were repelled from a prepatterned poly(ethylene glycol) surface, a well-defined colloidal array that included the proteins was created.

Recent studies on magnetism and magnetic materials have focused on magnetic nanostructures and their unique magnetic properties. In general, novel magnetic properties have been revealed by reducing the feature dimensions to certain characteristic length scales.[107] For example, nanoscale magnetic materials often exhibit superparamagnetic behavior. This disappearance of magnetization hinders the size reduction of magnetic domains, which is essential for the fabrication of high-density magnetic memory devices.[108] Moreover, an ordered nanostructure of magnetic materials is required for investigation of the mesoscopic effects induced by the confinement of magnetic materials in nanoscale domains.[109] Li et al. used CL to demonstrate that a sputtered cobalt thin film on a hexagonally packed colloid array can be potentially used in magnetic recording devices.[110] The sputtered magnetic materials were isolated due to the geometry of the arranged colloids, showing large hysteresis loop remanence. Similarly, Albrecht et al. also deposited a Co/Pd multilayer on a colloid surface, which exhibited magnetic anisotropy.[59] In this experiment, the coercivity was inversely proportional to the diameter of the colloid.

Since magnetic properties are strongly dependent on the domain size and the distance between domains, simple and direct CL is not suitable for controlling the feature scales of the nanopatterns. To resolve this, Weekes et al. proposed a modified CL technique for an isolated magnetic-dot array using RIE and electrodeposition.[53] Also, our group has re-

© 2006 Wiley-VCH Verlag GmbH & Co. KGaA, D-69451 Weinheim

ported a fabrication method for size- and shape-controllable magnetic metal arrays.[91] In these experiments, the coercivity and switching width of the isolated nanodot array were enhanced relative to those of a continuous magnetic film. In general, the vortex core on the center of disk-shaped magnetic materials tends to destabilize the vortex state, and also retards the switching speed during the reversal process.[111] Therefore, a magnetic nanoring structure shows a stable vortex state due to the absence of a destabilizing vortex core, and the fabrication of a well-organized nanoring array over a large area has been pursued by many researchers in recognition of its potential use for vertical magnetic random access memories.[112] For example, high-density nanoring arrays were created using CL, which controlled readily the geometric features of nanorings.[72,85]

5. Summary and Outlook

In this Review, we have discussed the general features and the state of the art of colloidal lithography. In principle, a colloid is a functional building block in itself ranging from several tens of nanometers to micrometer scales for 2D and 3D ordered architectures. CL is a new lithographic approach for creating 2D and 3D structures using the self-assembly of colloids. Spontaneous formation of well-ordered colloidal arrays provides lithographic masks or scaffolds for creating useful patterns. More importantly, modification of the self-assembled mask improves the versatility of CL in fabricating novel nanopatterns such as nanocups, hollow shells, and multifaceted materials.

In CL, however, it is necessary to solve the problems of defect formation during self-assembly and compatibility with photolithographic techniques for working devices. To this end, many studies have been undertaken, and notable results on defect-free colloidal arrays over a large area have been demonstrated using template-guided or interfacial self-assembly of colloids.[37,46,85] Also, the compatibility of CL with photolithography was improved by the spin-casting of colloids dispersed in a photocurable prepolymer solution.[43] The process of removing the defects in a colloidal array has been improved simultaneously with the development of colloidal patterning methods, and it is expected that defect-free colloid arrays or colloidal arrays with tolerable defect densities over large areas will be demonstrated in the near future.

Recently, studies on CL have created a new arena for multifunctional particles. Multifaceted and patterned particles with functional materials are of potential significance in emerging research fields including drug delivery, biodetection, and molecular electronics. Sculptured PS particles with controllable nanohole structures have been demonstrated. Further functionalization of the nanoholes with a variety of materials can facilitate the use of these multifaceted particles in patterned media and nanophotonics. Also, Yu et al. demonstrated a method for the direct patterning of lipid bilayer membranes of the surface of colloidal silica particles using photochemical lithography to generate asymmetric affinity for biomolecules.[113] This asymmetric affinity can be applied for further modification of the particle surface or for the display of biological signaling. Moreover, colloidal particles coated with magnetic materials have been utilized as molecular junctions for the measurement of charge transport.[114] The spherical shape of the colloid and the magnetic susceptibility of a coated magnet facilitated the magnetically directed assembly of the colloids between the electrodes. The applications noted above constitute only some of the potential of functionalized particles. Recent progress in colloidal science for tailoring the functional properties of colloidal particles by changing the composition, shape, and size of the particles is expected to allow for unprecedented versatility of colloidal arrays in a broad range of applications.

Acknowledgements

This work was supported by the Center for Nanoscale Mechatronics and Manufacturing of the 21st Century Frontier Research Program (M102 KN010002-05 K1401-00214). Partial support from the National R&D Project for Nano Science and Technology of the Ministry of Commerce, Industry and Energy, the BK21 program and the CUPS-ERC are also acknowledged.

[1] S. E. Lyshevski, *Nano- and Micro-Electromechanical Systems: Fundamentals of Nano- and Microengineering*, CRC Press, Boca Raton, FL, **2005**.
[2] J. A. Hoffnagle, W. D. Hinsber, M. Sanchez, F. A. Houle, *J. Vac. Sci. Technol. B* **1999**, *17*, 3306.
[3] R. L. Brainard, J. Cobb, C. A. Cutler, *J. Photopolym. Sci. Technol.* **2003**, *16*, 401.
[4] a) Y. Chen, A. Pepin, *Electrophoresis* **2001**, *22*, 187; b) D. Wouters, U. S. Schubert, *Angew. Chem.* **2004**, *116*, 2534; *Angew. Chem. Int. Ed.* **2004**, *43*, 2480; c) A. A. Tseng, *J. Micromech. Microeng.* **2004**, *14*, R15; d) A. A. Tseng, *Small* **2005**, *1*, 594; e) A. A. Tseng, *Small* **2005**, *1*, 924.
[5] S. Y. Chou, P. R. Krauss, P. J. Renstrom, *Science* **1996**, *272*, 85.
[6] Y. Xia, J. A. Rogers, K. E. Paul, G. M. Whitesides, *Chem. Rev.* **1999**, *99*, 1823.
[7] M. J. Fasolka, A. M. Mayes, *Annu. Rev. Mater. Res.* **2001**, *31*, 323.
[8] M. Park, C. Harrison, P. M. Chaikin, R. A. Register, D. H. Adamson, *Science* **1997**, *276*, 1401.
[9] a) M. R. Bockstaller, R. A. Mickiewicz, E. L. Thomas, *Adv. Mater.* **2005**, *17*, 1331; b) W. A. Lopes, H. M. Jaeger, *Nature* **2001**, *414*, 735; c) I. W. Hamley, *Nanotechnology* **2003**, *14*, R39.
[10] S. H. Kim, M. J. Misner, T. Xu, M. Kimura, T. P. Russell, *Adv. Mater.* **2004**, *16*, 226.
[11] a) Y. A. Vlasov, X.-Z. Bo, J. C. Sturm, D. J. Norris, *Nature* **2001**, *414*, 281; b) G.-R. Yi, V. N. Manoharan, S. Klein, K. R. Brzezinska, D. J. Pine, F. F. Lange, S.-M. Yang, *Adv. Mater.* **2002**, *14*, 1137; c) P. Jiang, J. F. Bertone, K. S. Hwang, V. L. Colvin, *Chem. Mater.* **1999**, *11*, 2132.
[12] R. Arshady, *Colloid Polym. Sci.* **1992**, *270*, 717.
[13] R. H. Ottewill, J. N. Shaw, *Kolloid Z. Z. Polym.* **1967**, *218*, 34.
[14] a) F. Sauzedde, F. Ganachaud, A. Elaïssari, C. Pichot, *J. Appl. Polym. Sci.* **1997**, *65*, 2331; b) P. H. Wang, C.-Y. Pan, *Colloid Polym. Sci.* **2002**, *280*, 152; c) A. H. Cardoso, C. A. P. Leite, F. Galembeck, *Langmuir* **1998**, *14*, 3187.
[15] a) D. Zou, V. Derlich, K. Gandhi, M. Park, L. Sun, D. Kriz, Y. D. Lee, G. Kim, J. J. Aklonis, R Salovey, *J. Polym. Sci. Part A:*

 © 2006 Wiley-VCH Verlag GmbH & Co. KGaA, D-69451 Weinheim

Polym. Chem. **1990**, *28*, 1909; b) D. Zou, S. Ma, R. Guan, M. Park, L. Sun, J. J. Aklonis, R. Salovey, *J. Polym. Sci. Part A: Polym. Chem.* **1992**, *30*, 137.
[16] D. Zou, L. Sun, J. J. Aklonis, R. Salovey, *J. Polym. Sci. Part A: Polym. Chem.* **1992**, *30*, 1463.
[17] *Dispersion polymerization in organic media* (Ed.: K. Barrette), Wiley, New York, **1975**.
[18] a) C. M. Tseng, Y. Y. Lu, M. S. El-Aasser, J. W. Vanderhoff, *J. Polym. Sci. Polym. Chem. Ed.* **1986**, *24*, 2995; b) S. M. Klein, V. N. Manoharn, D. J. Pine, F. F. Lange, *Colloid Polym. Sci.* **2003**, *282*, 7.
[19] W. Stöber, A. Fink, *J. Colloid Interface Sci.* **1968**, *26*, 62.
[20] a) A. K. Van Helden, J. W. Jansen, A. Vrij, *J. Colloid Interface Sci.* **1981**, *81*, 354; b) G. H. Bogush, M. A. Tracy, C. F. Zukoski, *J. Non-Cryst. Solids* **1988**, *104*, 95; c) E. Matijevic, *Langmuir* **1994**, *10*, 8; d) J. H. Zhang, P. Zhan, Z. L. Wang, W. Y. Zhang, N. B. Ming, *J. Mater. Res.* **2003**, *18*, 649.
[21] a) M. Ueda, H.-B. Kim, K. Ichimura, *J. Mater. Chem.* **1994**, *4*, 883; b) W. Wang, B. Gu, L. Liang, W. Hamilton, *J. Phys. Chem. B* **2003**, *107*, 3400.
[22] W. B. Russel, D. A. Saville, W. R. Schowalter, *Colloidal dispersions*, Cambridge University Press, Cambridge, **1989**.
[23] J. Visser, *Surface and Colloid Science*, Vol. *8*, Wiley, New York **1976**.
[24] N. D. Denkov, O. D. Velev, P. A. Kralchevsky, I. B. Ivanov, H. Yoshimura, K. Nagayama, *Langmuir* **1992**, *8*, 3183.
[25] A. S. Dimitrov, K. Nagayama, *Langmuir* **1996**, *12*, 1303.
[26] M. Kondo, K. Shinozaki, L. Bergstrom, N. Mizutani, *Langmuir* **1995**, *11*, 394.
[27] H. H. Wickman, J. N. Korley, *Nature* **1998**, *393*, 445.
[28] R. Aveyard, J. H. Clint, D. Nees, V. N. Paunov, *Langmuir* **2000**, *16*, 1969.
[29] T. S. Horozov, R. Aveyard, J. H. Clint, B. P. Binks, *Langmuir* **2003**, *19*, 2822.
[30] K. U. Fulda, B. Tieke, *Adv. Mater.* **1994**, *6*, 288.
[31] a) M. Trau, S. Sankaran, D. A. Saville, I. A. Aksay, *Nature* **1995**, *374*, 437; b) M. Trau, D. A. Saville, I. A. Aksay, *Science* **1996**, *272*, 706; c) R. C. Hayward, D. A. Saville, I. A. Aksay, *Nature* **2000**, *404*, 56; d) Y. Solomentsev, M. Bohmer, J. L. Anderson, *Langmuir* **1997**, *13*, 6058.
[32] a) A. E. Larsen, D. G. Grier, *Phys. Rev. Lett.* **1996**, *76*, 3862; b) T. Gong, D. W. M. Marr, *Langmuir* **2001**, *17*, 2301; c) S. O. Lumsdon, E. W. Kaler, O. D. Velev, *Langmuir* **2004**, *20*, 2108.
[33] P. J. Sides, *Langmuir* **2001**, *17*, 5791.
[34] A. L. Rogach, N. A. Kotov, D. S. Koktysh, J. W. Ostrander, G. A. Ragoisha, *Chem. Mater.* **2000**, *12*, 2721.
[35] E. Kumacheva, R. K. Golding, M. Allard, E. H. Sargent, *Adv. Mater.* **2002**, *14*, 221.
[36] A. Winkleman, B. D. Gates, L. S. Mccarty, G. M. Whitesides, *Adv. Mater.* **2005**, *17*, 1507.
[37] a) E. Kim, Y. Xia, G. M. Whitesides, *Adv. Mater.* **1996**, *8*, 245; b) B. Gates, D. Qin, Y. Xia, *Adv. Mater.* **1999**, *11*, 466; c) G. A. Ozin, S. M. Yang, *Adv. Funct. Mater.* **2001**, *11*, 95.
[38] a) J. Aizenberg, P. V. Braun, P. Wiltzius, *Phys. Rev. Lett.* **2000**, *84*, 2997; b) F. Fan, K. J. Stebe, *Langmuir* **2004**, *20*, 3062.
[39] a) H. P. Zheng, I. Lee, M. F. Rubner, P. T. Hammond, *Adv. Mater.* **2002**, *14*, 569; b) H. Y. Koo, D. K. Yi, S. J. Yoo, D.-Y. Kim, *Adv. Mater.* **2004**, *16*, 274; c) Z. Adamczyk, M. Zembala, B. Siwek, P. Warszynski, *J. Colloid Interface Sci.* **1990**, *140*, 123.
[40] Y. Xia, Y. Yin, Y. Lu, J. McLellan, *Adv. Funct. Mater.* **2003**, *13*, 907.
[41] a) K. P. Velikov, C. G. Christova, R. P. A. Dullens, A. van Blaaderen, *Science* **2002**, *296*, 106; b) H. Cong, W. Cao, *J. Phys. Chem. B* **2005**, *109*, 1695; c) V. Kitaev, G. A. Ozin, *Adv. Mater.* **2003**, *15*, 75; d) D. Wang, H. Möhwald, *Adv. Mater.* **2004**, *16*, 244.
[42] J. C. Hulteen, R. P. van Duyne, *J. Vac. Sci. Technol. A* **1995**, *13*, 1553.
[43] a) P. Jiang, M. F. McFarland, *J. Am. Chem. Soc.* **2004**, *126*, 13778; b) P. Jiang, M. F. McFarland, *J. Am. Chem. Soc.* **2005**, *127*, 3710.
[44] a) H. W. Deckman, J. H. Dunsmuir, *Appl. Phys. Lett.* **1982**, *41*, 377; b) U. C. Fischer, H. P. Zingsheim, *J. Vac. Sci. Technol.* **1981**, *19*, 881.
[45] J. C. Hulteen, D. A. Treichel, M. T. Smith, M. L. Duval, T. R. Jensen, R. P. van Duyne, *J. Phys. Chem. B* **1999**, *103*, 3854.
[46] K. Kempa, B. Kimball, J. Rybczynski, Z. P. Huang, P. F. Wu, D. Steeves, M. Sennett, M. Giersig, D. V. G. L. N. Rao, D. L. Carnahan, D. Z. Wang, J. Y. Lao, W. Z. Li, Z. F. Ren, *Nano Lett.* **2003**, *3*, 13.
[47] a) Z. F. Ren, Z. P. Huang, J. W. Xu, J. H. Wang, P. Bush, M. P. Siegal, P. N. Provencio, *Science* **1998**, *282*, 1105; b) Y. Tu, Z. P. Huang, D. Z. Wang, J. G. Wen, Z. F. Ren, *Appl. Phys. Lett.* **2002**, *80*, 4018.
[48] X. Wang, C. J. Summers, Z. L. Wang, *Nano Lett.* **2004**, *4*, 423.
[49] J. Pacifico, D. Gomez, P. Mulvaney, *Adv. Mater.* **2005**, *17*, 415.
[50] J. G. C. Veinot, H. Yan, S. M. Smith, J. Cui, Q. Huang, T. J. Marks, *Nano Lett.* **2002**, *2*, 333.
[51] C.-W. Kuo, J.-Y. Shiu, P. Chen, *Chem. Mater.* **2003**, *15*, 2917.
[52] C.-W. Kuo, J.-Y. Shiu, Y.-H. Cho, P. Chen, *Adv. Mater.* **2003**, *15*, 1065.
[53] S. M. Weekes, F. Y. Ogrin, W. A. Murray, *Langmuir* **2004**, *20*, 11208.
[54] a) F. A. Denis, P. Hanarp, D. S. Sutherland, J. Gold, C. Mustin, P. G. Rouxhet, Y. F. Dufrêne, *Langmuir* **2002**, *18*, 819; b) D. S. Sutherland, M. Broberg, H. Nygren, B. Kasemo, *Macromol. Biosci.* **2001**, *1*, 270.
[55] R. Michel, I. Reviakine, D. Sutherland, C. Fokas, G. Csucs, G. Danuser, N. D. Spencer, M. Textor, *Langmuir* **2002**, *18*, 8580.
[56] F. A. Denis, P. Hanarp, D. S. Sutherland, Y. F. Dufrêne, *Langmuir* **2004**, *20*, 9335.
[57] B. J.-Y. Tan, C.-H. Sow, K.-Y. Lim, F.-C. Cheong, G.-L. Chong, A. T.-S. Wee, C.-K. Ong, *J. Phys. Chem. B* **2004**, *108*, 18575.
[58] A. Valsesia, P. Colpo, M. M. Silvan, T. Meziani, G. Ceccone, F. Rossi, *Nano Lett.* **2004**, *4*, 1047.
[59] M. Albrecht, G. Hu, I. L. Guhr, T. C. Ulbrich, J. Boneberg, P. Leiderer, G. Schatz, *Nat. Mater.* **2005**, *4*, 203.
[60] a) P. F. Carcia, A. D. Meinhaldt, A. Suna, *Appl. Phys. Lett.* **1985**, *47*, 178; b) T. Suzuki, *Scr. Metall. Mater.* **1995**, *33*, 1609.
[61] a) T. Cassagneau, F. Caruso, *Adv. Mater.* **2002**, *14*, 34; b) P. N. Bartlett, P. R. Birkin, M. A. Ghanem, C.-S. Toh, *J. Mater. Chem.* **2001**, *11*, 849; c) T. Sumida, Y. Wada, T. Kitamura, S. Yanagida, *Chem. Commun.* **2000**, 1613.
[62] a) T. W. Ebbesen, H. J. Lezec, H. F. Ghaemi, *Nature* **1998**, *391*, 667; b) Y. Xia, J. Rogers, K. E. Paul, G. M. Whitesides, *Chem. Rev.* **1999**, *99*, 1823; c) J. Ji, X. Li, L. T. Canham, J. L. Coffer, *Adv. Mater.* **2002**, *14*, 41.
[63] S. Han, X. Shi, F. Zhou, *Nano Lett.* **2002**, *2*, 97.
[64] J. C. Garno, N. A. Amro, K. Wadu-Mesthrige, G.-Y. Liu, *Langmuir* **2002**, *18*, 8186.
[65] F. Sun, W. Cai, Y. Li, B. Cao, F. Lu, G. Duan, L. Zhang, *Adv. Mater.* **2004**, *16*, 1116.
[66] a) T. Suntola, *Mater. Sci. Rep.* **1989**, *4*, 261; b) M. Leskela, M. Ritala, *Thin Solid Films* **2002**, *409*, 138.
[67] X. D. Wang, E. Graugnard, F. S. King, Z. L. Wang, C. J. Summers, *Nano Lett.* **2004**, *4*, 2223.
[68] Mikrajuddin, F. Iskandar, K. Okuyama, *Adv. Mater.* **2002**, *14*, 930.
[69] J. C. Love, B. D. Gates, D. B. Wolfe, K. E. Paul, G. M. Whitesides, *Nano Lett.* **2002**, *2*, 891.
[70] Y. Lu, G. L. Liu, J. Kim, Y. X. Mejia, L. P. Lee, *Nano Lett.* **2005**, *5*, 119.

 © 2006 Wiley-VCH Verlag GmbH & Co. KGaA, D-69451 Weinheim

[71] J. Aizpurua, P. Hanarp, D. S. Sutherland, M. Kall, G. W. Bryant, F. J. Garcia de Abajo, *Phys. Rev. Lett.* **2003**, *90*, 057 401.
[72] F. Q. Zhu, D. Fan, S. Zhu, J.-G. Zhu, R. C. Cammarata, C.-L. Chien, *Adv. Mater.* **2004**, *16*, 2155.
[73] J. M. McLellan, M. Geissler, Y. Xia, *J. Am. Chem. Soc.* **2004**, *126*, 10 830.
[74] M. Geissler, J. M. McLellan, J. Chen, Y. Xia, *Angew. Chem.* **2005**, *117*, 3662; *Angew. Chem. Int. Ed.* **2005**, *44*, 3596.
[75] a) F. Keller, M. S. Hunter, D. L. Robinson, *J. Electrochem. Soc.* **1953**, *100*, 411; b) J. W. Diggle, T. C. Downie, C. W. Goulding, *Chem. Rev.* **1969**, *69*, 365; c) S. Kawai, R. Ueda, *J. Electrochem. Soc.* **1975**, *122*, 32.
[76] S. Fournier-Bidoz, V. Kitaev, D. Routkevitch, I. Manners, G. A. Ozin, *Adv. Mater.* **2004**, *16*, 2193.
[77] X. Chen, Z. Sun, L. Zheng, Z. Chen, Y. Wang, N. Fu, K. Zhang, X. Yan, H. Liu, L. Jiang, B. Yang, *Adv. Mater.* **2004**, *16*, 1632.
[78] D.-G. Choi, S. G. Jang, H. K. Yu, S.-M. Yang, *Chem. Mater.* **2004**, *16*, 3410.
[79] a) E. Hutter, J. H. Fendler, *Adv. Mater.* **2004**, *16*, 1685; b) A. J. Haes, R. P. van Duyne, *Anal. Bioanal. Chem.* **2004**, *379*, 920.
[80] a) Z. Q. Tian, B. Ren, D. Y. Wu, *J. Phys. Chem. B* **2002**, *106*, 9463; b) K. Kneipp, H. Kneipp, I. Itzkan, *J. Phys. Condens. Matter* **2002**, *14*, R597.
[81] J. I. Martin, J. Nogues, K. Liu, J. L. Vicent, I. K. Schuller, *J. Magn. Magn. Mater.* **2003**, *256*, 449.
[82] a) C. L. Haynes, R. P. van Duyne, *J. Phys. Chem. B* **2001**, *105*, 5599; b) C. L. Haynes, A. D. Mcfarland, M. T. Smith, J. C. Hulteen, R. P. van Duyne, *J. Phys. Chem. B* **2002**, *106*,1898.
[83] D. W. van Krevelen, *Properties of polymers*, 3rd ed., Elsevier, New York, **1990**.
[84] P. Hanarp, M. Kall, D. S. Sutherland, *J. Phys. Chem. B* **2003**, *107*, 5768.
[85] A. Kosiorek, W. Kandulski, H. Glaczynska, M. Giersig, *Small* **2005**, *1*, 439.
[86] D. L. J. Vossen, D. Fific, J. Penninkhof, T. van Dillen, A. Polman, A. van Blaaderen, *Nano Lett.* **2005**, *5*, 1175.
[87] C. Haginoya, M. Ishibashi, K. Koike, *Appl. Phys. Lett.* **1997**, *71*, 2934.
[88] a) F. D. Egitto, L. J. Matienzo, *IBM J. Res. Dev.* **1994**, *38*, 423; b) Q. He, Z. Liu, P. Xiao, R. Liang, N. He, Z. Lu, *Langmuir* **2003**, *19*, 6982; c) H. M. Powell, J. J. Lannutti, *Langmuir* **2003**, *19*, 9071.
[89] D.-G. Choi, H. K. Yu, S. G. Jang, S.-M. Yang, *J. Am. Chem. Soc.* **2004**, *126*, 7019.
[90] a) Y. Yin, Y. Xia, *J. Am. Chem. Soc.* **2003**, *125*, 2048; b) Y. Yin, Y. Xia, *Adv. Mater.* **2002**, *14*, 605; c) D.-G. Choi, H. K. Yu, S. G. Jang, S.-M. Yang, *Chem. Mater.* **2003**, *15*, 4169.
[91] D.-G. Choi, S. Kim, S. G. Jang, S.-M. Yang, J.-R. Jeong, S.-C. Shin, *Chem. Mater.* **2004**, *16*, 4208.
[92] a) J. H. Moon, W.-S. Kim, J.-W. Ha, S. G. Jang, S.-M. Yang, J. K. Park, *Chem. Commun.* **2005**, 4107; b) J. H. Moon, S. G. Jang, J.-M. Lim, S.-M. Yang, *Adv. Mater.* **2005**, *17*, 2559.
[93] D.-G. Choi, S. Kim, E. Lee, S.-M. Yang, *J. Am. Chem. Soc.* **2005**, *127*, 1636.
[94] D.-G. Choi, S. G. Jang, S. Kim, E. Lee, C.-S. Han, S.-M. Yang, *Adv. Funct. Mater.* **2006**, *16*, 33.
[95] a) E. Hutter, J. H. Fendler, *Adv. Mater.* **2004**, *16*, 1685; b) P. Mayer, *Mater. Res. Soc. Symp. Proc.* **1997**, *463*, 57; c) R. Elghanian, J. J. Storhoff, R. C. Mucic, R. L. Letsinger, C. A. Mirkin, *Science* **1997**, *277*, 1078; d) A. T. Wooley, C. Guillemette, C. L. Cheung, D. E. Housman, C. M. Lieber, *Nat. Biotechnol.* **2000**, *18*, 760; e) E. Braun, Y. Eichen, U. Sivan, G. Ben-Yoseph, *Nature* **1998**, *391*, 775; f) R. P. Andes, T. Bein, M. Dorogi, S. Feng, J. I. Henderson, C. P. Kubiak, W. Mahoney, R. G. Osifchin, R. Reifenberger, *Science* **1996**, *272*, 1323.
[96] a) S. A. Maier, M. L. Brongersma, P. G. Kik, S. Meltzer, A. A. G. Requicha, H. A. Atwater, *Adv. Mater.* **2001**, *13*, 1501; b) W. L. Barnes, A. Dereux, T. W. Ebbesen, *Nature* **2003**, *424*, 824; c) F. Frederix, J.-M. Friedt, K.-H. Choi, W. Laureyn, A. Campitelli, D. Mondelaers, G. Maes, G. Borghs, *Anal. Chem.* **2003**, *75*, 6894; d) A. Curry, G. Nusz, A. Chilkoti, A. Wax, *Opt. Express* **2005**, *13*, 2668.
[97] E. M. Hicks, S. Zou, G. C. Schatz, K. G. Spears, R. P. van Duyne, L. Gunnarsson, T. Rindzevicius, B. Kasemo, M. Kall, *Nano Lett.* **2005**, *5*, 1065.
[98] C. L. Haynes, A. D. McFarland, L. Zhao, R. P. van Duyne, G. C. Schatz, L. Gunnarsson, J. Prikulis, B. Kasemo, M. Käll, J. Phys, *J. Phys. Chem. B* **2003**, *107*, 7337.
[99] K. L. Kelly, E. Coronado, L. Zhao, G. C. Schatz, *J. Phys. Chem. B* **2003**, *107*, 668.
[100] B. Lamprecht, G. Schider, R. T. Lechner, H. Ditlbacher, J. R. Krenn, A. Leitner, F. R. Aussenegg, *Phys. Rev. Lett.* **2000**, *84*, 4721.
[101] a) C. Charnay, A. Lee, S.-Q. Man, C. E. Moran, C. Radloff, R. K. Bradley, N. J. Halas, *J. Phys. Chem. B* **2003**, *107*, 7327; b) J. Liu, A. I. Maaroof, L. Wieczorek, M. B. Cortie, *Adv. Mater.* **2005**, *17*, 1276.
[102] A. J. Haes, L. C. William, L. Klein, R. P. Van Duyne, *J. Am. Chem. Soc.* **2005**, *127*, 2264.
[103] K. Kneipp, H. Kneipp, I. Itzkan, R. R. Dasari, M. S. Feld, *J. Phys. Condens. Matter* **2002**, *14*, R597.
[104] K. Kneipp, H. Kneipp, V. B. Kartha, R. Manoharan, G. Deinum, I. Itzkan, R. R. Dasari, M. S. Feld, *Phys. Rev. E* **1998**, *57*, R6281.
[105] M. Veiseh, M. H. Zareie, M. Q. Zhang, *Langmuir* **2002**, *18*, 6671.
[106] C. Wang, Y. Zhang, *Adv. Mater.* **2005**, *17*, 150.
[107] J. I. Martin, J. Nogues, K. Liu, J. L. Vicent, I. K. Schuller, *J. Magn. Magn. Mater.* **2003**, *256*, 449.
[108] A. Moser, K. Takano, D. T. Margulis, M. Albrecht, Y. Sonobe, Y. Ikeda, S. Sun, E. E. Fullerton, *J. Phys. D* **2002**, *35*, R157.
[109] a) E. Grochowski, D. Thompson, *IEEE Trans. Magn.* **1994**, *30*, 3797; b) E. Grochowski, R. F. Hoyt, *IEEE Trans. Magn.* **1996**, *32*, 1850; c) K. O'Grady, H. Laidler, *J. Magn. Magn. Mater.* **1999**, *200*. 616.
[110] S. P. Li, W. S. Lew, Y. B. Xu, A. Hirohata, A. Samad, F. Baker, J. A. C. Bland, *Appl. Phys. Lett.* **2000**, *76*, 748.
[111] a) M. Klaui, C. A. F. Vaz, L. Lopez-Diaz, J. A. C. Bland, *J. Phys. Condens. Matter* **2003**, *15*, R985; b) S. P. Li, D. Peyrade, M. Natali, A. Lebib, Y. Chen, U. Ebels, L. D. Buda, K. Ounadjela, *Phys. Rev. Lett.* **2001**, *86*, 1102; c) J. Rothman, M. Klaui, L. Lopez-Diaz, C. A. F. Vaz, A. Bleloch, J. A. C. Bland, Z. Cui, R. Speaks, *Phys. Rev. Lett.* **2001**, *86*, 1098.
[112] J. G. Zhu, Y. Zheng, G. A. Prinz, *J. Appl. Phys.* **2000**, *87*, 6668.
[113] C.-H. Yu, A. N. Parikh, J. T. Groves, *Adv. Mater.* **2005**, *17*, 1477.
[114] D. P. Long, C. H. Patterson, M. H. Moore, D. S. Seferos, G. C. Bazan, J. G. Kushmerick, *Appl. Phys. Lett.* **2005**, *86*, 153 105.

Received: October 12, 2005

 © 2006 Wiley-VCH Verlag GmbH & Co. KGaA, D-69451 Weinheim